Assessing the economic and energy efficiency for multi-energy virtual power plants in regulated markets: a case study in Egypt

Sustainable Cities and Society 83 (2022) 103968

Contents lists available at ScienceDirect

Sustainable Cities and Society

journal homepage: www.elsevier.com/locate/scs

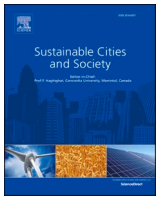

Assessing the economic and energy efficiency for multi-energy virtual power plants in regulated markets: A case study in Egypt

Ahmed Hany Elgamal *, Maria Vahdati, Mehdi Shahrestani

School of the Built Environment, University of Reading, Reading, RG6 6DF, UK

ARTICLE INFO

Keywords:
Energy markets
Energy trading policy
Solar PV
CCHP
Virtual power plant

ABSTRACT

This paper investigates the design and operation management of VPPs in regulated markets. A new framework based on profit maximization objective function is presented in this study. The hypotheses of this research is that considering profit as an objective function would yield a more realistic and optimal sizes compared to Cost of Energy (COE) minimization approach adopted in literature. The analyzed VPP aggregates solar PV units, CCHP supplying power and thermal energy, Battery storage system and thermal energy storage system. The system is formulated in an optimization model fed by energy demand profile, prices and inputs for solar power (irradiance and weather data). The objective function is formulated based on maximization of profit of the VPP selling power to the grid by Power Purchase Agreement (PPA), selling power to consumers at the public electricity tariff, and selling thermal energy at an assumed constant tariff. CCHP non-linear part-load efficiency is also considered in the model, accordingly, Genetic Algorithm (GA) is employed to solve the optimization. Results of the optimally configured model achieved 36% improvement in COE compared to literature. Solar power contributed by 31% from the total produced energy without imbalance, grid power contributed by 4%, and CO2 emissions reduced by 47% compared to full dependency on the grid. Statistical relationships were drawn showing the relationship between profit, energy and exergy efficiencies versus different CCHP capacities. In addition, analysis is provided for the efficiencies' relation with the dumped heat from the CCHP.

1. Introduction

After the recent events of COP26 and commitments to cut emissions, the need became clearer to deploy more renewable energy in the electricity grids (UKCOP26, 2021), but their integration without proper planning and management, eventually could disturb the grid and cause blackouts (McGreevy, et al., 2021). Decentralized energy resources (DERs), where energy is produced at consumers sites, are found to be one of the most economic and energy efficient ways for the deployment and exploration of renewable energy (Dio, et al., 2015). The literature proved that DERs, especially when aggregated, are beneficial for profit maximization (Calvillo, et al., 2016). A particular form of aggregated DERs, namely Virtual Power Plant (VPP), is the focus of the research.

A concept called Virtual Power plant have been developing through the past 2 decades, proposed with various business models "deregulated energy markets" where free energy trading with the grid is allowed and wholesale energy market is deployed (Foroughi, et al., 2021). However, modeling VPPs in the other type which is "regulated" markets, has been overlooked in literature. Technical challenges of renewables penetration in the grid have been addressed in literature, such as grid stability caused by intermittency and high capital costs compared to conventional power plants. With continuous large-scale increase of renewables, there will be a need to keep thermal power plants on reserve as back-up (Martinopoulos & Bassiliades, 2019). VPPs are believed to mitigate renewables intermittency problems since they can aggregate renewable and dispatchable plants and offer a higher level of operational flexibility. In both regulated and deregulated markets, power plants could have a power purchase agreement (PPA) with the buyer, where the buyer agrees to buy from an IPP a contracted volume of energy at a predefined price (RE-Source, 2020). PPAs differ in forms but in this research we are assuming a "pay as generated" form which enables a renewable power plant to sell what it could to the grid.

Literature could be classified by the financial objective of the design and operation management of VPP in 2 main market cases. Those market cases are either the deregulated market, where the main objective function is to maximize profit from trading in day-ahead and/or balancing markets (Nosratabadi, et al., 2017), or the regulated market where the main objective is to minimize the COE (Diab, et al., 2019). These 2 categories will be separately reviewed, however, the main target

* Corresponding author.
E-mail addresses: a.h.elgamal@pgr.reading.ac.uk (A.H. Elgamal), m.m.vahdati@reading.ac.uk (M. Vahdati), m.shahrestani@reading.ac.uk (M. Shahrestani).

https://doi.org/10.1016/j.scs.2022.103968
Received 4 February 2022; Received in revised form 27 May 2022; Accepted 27 May 2022
Available online 28 May 2022

Nomenclature

P_{CCHP}	CCHP output power, kW
$\omega 1$, $\omega 2$	Weighing factor for multi-objective function
Q_{CHW}	Cooling output from AC, kW
Q_{HW}	Heat output converted from waste heat, kW
$\dot{m}_f$	CCHP input fuel flow rate, m^3/hr
$\dot{m}_{f-ac}$	AC input fuel flow rate, m^3/hr
T_o	Ambient Temperature, K
T_{CHW}	Chilled water Temperature, K
T_{HW}	Heating water Temperature, K
SU	CCHP Start-up binary
v_t	CCHP Start-up binary
u_{grid}	Binary for energy trading with grid (Buying:1; selling: 0)
$P_{gridbuy}$	Purchased power from the grid, kW
$P_{gridsell}$	Sold power to the grid, kW
$P_{gridbuy\_max,t}$	Upper bound for energy purchased from the grid
$P_{gridsell\_max,t}$	Upper bound for sold energy to the grid
P_{PV}	Solar PV Power, kW
$u_{BSS-disch}$	Binary for BSS discharging
u_{BSS-ch}	Binary for BSS charging
u_{cchp}	Binary for ON/OFF status of the CCHP
P_{ch}	BSS charged power, kW
P_{disch}	BSS discharged power, kW
P_{demand}	Electricity demand, kW
η_{TES}	TES roundtrip efficiency, %
E_{CHW-TS}	State of charge of cold water storage, kW
E_{HW-TS}	State of charge of hot water storage, kW
η_{charge}, $\eta_{discharge}$	BSS roundtrip efficiency, %
η_{PV}	Solar PV module overall efficiency, %
η_r	Solar PV module reference efficiency
A_{PV}	Solar PV module installed area, m^2
G	Solar irradiation, kW/m2
T_c	Solar PV cell temperature, K
$NOCT$	Nominal operating cell temperature, K
β	PV pannel tilt angle
T_{ref}	Solar PV cell reference temperature, (25 K)
γ	Power to heat ratio
η_{CCHPe}	CCHP electrical efficiency, %
$\eta_{CCHPe\_nominal}$	CCHP nominal electrical efficiency, %
$Q_{recovered}$	Total recovered heat from CCHP, kW
Q_{exh}	Exhaust (high grade) waste heat from CCHP, kW
Q_{jw}	Jacket cooling water & Oil (low grade) waste heat from CCHP, kW
F	CO2 emissions, kg
μ_{CO2}	CO2 emission factor, kg/kWh
LHV_f	Lower heating value of fuel, kWh/m^3
HHV_f	Higher heating value of fuel, kWh/m^3

Subscripts

t	Current time step
T	Time duration
NG	Natural gas flow rate
c	COP of AC at cooling mode
h	COP of AC at heating (heat pump) mode

Acronyms

BSS	Battery Storage System
CCHP	Combined Cooling Heat and Power
ICE	Internal combustion engine
PPA	Power Purchase Agreement
COP	Coefficient of Performance
TES	Thermal Energy Storage
COE	Cost of energy
LCOE	Levelized Cost of Energy
DER	Distributed Energy Resources
GA	Genetic Algorithm
PSO	Particle Swarm Optimization
WOA	Whale optimization algorithm
AC	Absorption Chiller
COP	Coefficient of Performance
SOC	State of Charge of Storage systems

of this research is to analyze in depth the case of the regulated market where literature overlooked the consideration of profit formulation in the objective function.

2. Literature review

2.1. Deregulated market

In deregulated markets, VPPs act as a mediator which could manage the operation of multiple power plants of different owners (Next Kraftwerke, 2021). Studies proposed different methods for profit maximization. Pandžić et al. (2013) proposed a two-stage Mixed integer linear programming stochastic optimization for a VPP in Croatia, aiming to maximize the VPP profit from trading in the day-ahead and balancing markets regardless of matching the VPP output with the load. The VPP case study consists of a 9.6 MW wind farm, 5.67 MW thermal power plant and 40 MWh pumped hydro storage scheme. Thermal plant's efficiency is taken as constant, and operating cost with part-load operation is linearized with piecewise linear approximation. Results showed that the VPP is following price signals without consideration to actual energy demand, and assumed that all surpluses sold to the balancing market will be accepted by the grid. Zamani et al. (2016) proposed a two-stage Point Estimate Method (PEM) optimization algorithm for a VPP in Canada, to maximize its profits from bidding the scheduled CHP power to the day-ahead market and the available reserve capacity of the VPP to the spinning reserve markets. The VPP consisted of Wind turbine, Solar PV units, CHP, electric boiler, demand response resources (controlled load), electrical storage and thermal storage units. The efficiency of CHP is considered constant without part-load efficiency modeling, which causes a big uncertainty in results. Results showed that VPP hourly profit profile is following the hourly energy price, by prioritizing the economic benefit over performance, surplus heat exceeding thermal demand existed and is dumped without utilization.

Maleki et al. (2017) used GA algorithm to maximize the net profit of a grid-connected VPP in Iran, aggregating 36 × 110 W Solar PV units, 1 kW wind turbine, 2 kW hydrogen-powered fuel cell from which heat is recovered and sold to the consumer, hence acting as a CHP, to cover the electricity and heat demand of a single household in Iran. Results showed a large dependency on the grid, the system purchases 1.2 kW for 8 hours when prices are low, and it secures savings in energy costs but did not achieve attractive profits. Payback period is not discussed to justify the system costs, and simulation is conducted in winter without discussing the operation performance in summer where cooling demand is dominant. Wang et al. (2015) aggregated existing power plants in Finland consisting of 2 biomass CHP plants (12.5 MW/38 MWth, 11 MW/36 MWth), 1 natural-gas CHP (8.4 MW/17 MWth), 2 boilers (62 MW and 70 MW), 1 solar thermal plant having 10,000 m2 solar panels, 1 × 10,000 m3 thermal storage tank and electric energy storage system (non-specified type nor size), aiming to minimize the power and heat net generation costs. Their results showed that CHPs are more dominant in

Table 1
Literature review summary.

Reference	Aim	Objective	Location	Efficiency function	Market Type	Energy demand covered	Key Findings
(Pandžić, et al., 2013)	Dispatch optimization	Max. Profit	Croatia	Constant/ Linear	Deregulated	Power	Presented a probabilistic optimization method following day-ahead and balancing markets
(Zamani, et al., 2016)	Dispatch optimization	Max. Profit	Canada	Constant/ Linear	Deregulated	Heating & Power	Power dispatch is following price signals regardless of demand, high surplus is generated and assumed accepted and bought by balancing market.
(Maleki, et al., 2017)	Dispatch optimization	Max. Profit	Iran	Constant/ Linear	Deregulated	Heating, Power	Dispatch optimization is simulated with GA and PSO algorithms, GA achieved better results. Daily profit achieved was 0.39$ from electricity and thermal energy sales, due to large dependency on power purchase from the grid.
(Kumara, et al., 2015)	Dispatch optimization	Max. Profit	Europe	Constant/ Linear	Deregulated	Power	Additive Increase Multiplicative Decrease (AIMD) is tested against a proposed modified case of the same algorithm, and 3.27% saving in cost of generation was achieved with the modified method.
(Zeng, et al., 2020)	Dispatch optimization	Max. Profit	Singapore	Constant/ Linear	Deregulated	Cooling, Heating, Power	Low deviation between actual dispatched power in real-time generation and scheduled in the day-ahead market High dependency on the grid is almost present during all time steps, as well as large portion of cooling demand is covered by traditional air conditioners
(Xu, et al., 2021)	Dispatch optimization	Max. Profit	China	Constant/ Linear	Deregulated	Cooling, Power	Electric vehicles' inclusion in the VPP improved the profit by reducing the need to dispatch the gas turbine for a significant duration.
(Zhang, et al., 2020)	Dispatch optimization	Max. Profit	China	Constant/ Linear	Deregulated	Cooling, Heating, Power	Improved heat load following CCHP achieved optimal objective function Improved artificial bee colony algorithm achieved better results compared with PSO and Whale optimization algorithm Dependency on the grid is more than 50% (observed from power balance diagrams)
(Diab, et al., 2019)	Sizing	Min. COE	Egypt	Constant/ Linear	Regulated	Power	WOA achieved optimality. Achieved a COE of 0.218 $/kWh. No actual energy prices are considered nor thermal demand coverage.
(Barakat, et al., 2016)	Sizing	Min. NPC	Egypt	Constant/ Linear	Regulated	Power	8% of the energy demand is covered by the grid. Selling energy to consumers is not discussed. Thermal demand is not considered.
(Elkadeem, et al., 2020)	Sizing	Min NPC & Min GHG	Egypt	Constant/ Linear	Regulated	Power	Achieved a COE of 0.15$/kWh Energy exchange with the grid is not considered nor thermal demand coverage.
(Abo-Elyousr & Elnozahy, 2018)	Sizing	Min. COE Min. GHG	Egypt	Constant/ Linear	Regulated	Power	Achieved a COE of 0.538 $/kWh for the min. COE objective, 21.92 $/kWh for the min. GHG objective, and 1.082 $/kWh for the multi-objective.
(El-Sattar, et al., 2021)	Sizing	Min. COE	Egypt	Constant/ Linear	Regulated	Power	Achieved a COE of 0.339 $/kWh
(El-Sattar, et al., 2021)	Sizing	Min. COE	Egypt	Constant/ Linear	Regulated	Power	Achieved a COE of 0.11 $/kWh
(Ramli, et al., 2018)	Sizing	Min. COE	KSA	Constant/ Linear	Regulated	Power	Achieved a COE of 0.05 $/kWh
(Cano, et al., 2020)	Sizing	Min. COE	Ecuador	Constant/ Linear	Regulated	Power	Achieved a COE of 0.18 $/kWh
(Mandal, et al., 2018)	Sizing	Min. COE	Bangladesh	Constant/ Linear	Regulated	Power	Achieved a COE of 0.37 $/kWh

covering power and thermal demand, while solar thermal power was not significant. Kumara et al. (2015) proposed two-stage optimization algorithm to schedule a micro-grid consisting of multiple DERs and proved to be powerful in predicting uncertainties and achieved a reduction in costs by 3.27% over 24 hours period. However, the study is purely optimizing based on the plant generation costs and not focusing on power plant profits.

Zeng et al. (2020) presented a high resolution (5-mins time step) real-time optimization method for a grid-connected hybrid system in Singapore, consisting of 1 MW Micro-turbine, 187.8 kW solar PV, wind turbines, batteries, thermal storage, 2000 kW waste heat boiler, 1000 kW gas boilers and 500 MW electric refrigerator, 2000 kW lithium bromide absorption chiller, to cover space cooling and heating, refrigeration, and power demand. The study highlighted the importance of short-term forecasting to reduce the deviation between scheduled power in the day-ahead market and real-time energy demand, which might occur due to renewables intermittency. Zeng et al. (2020) did not evaluate the economic viability of the system in terms of capital cost and payback period as there are several components in the integrated system. In addition, efficiencies of the systems are treated as constants which do not accurately reflect the fuel consumption and cost accordingly, also a large portion of space cooling demand was covered by household air conditioners.

Xu et al. (2021) proposed a receding horizon approach in a VPP in China, consisting of a gas turbine, solar PV units, air conditioners with thermal storage units, and Electric vehicles. The optimization is solved over a defined horizon and uses the actual data from the previous time step to reduce the solar power forecasting horizon and error. The model is beneficial to reduce uncertainty risks however, the optimization objective is set to minimize the generation costs and maximize the profit from grid exchange without including actual regulation on penalty costs from the imbalance between the scheduled and actual power. In

addition, efficiencies are also treated as constants and the optimization is solved as a mixed integer linear programming. Zhang et al. (2020) studied the impact of solar PV plant on its backup CCHP plant in a microgrid in China, and proposed a multi-objective optimization for plants dispatch based on an improved artificial bee colony algorithm. The aggregated system consists of solar PV Units, Micro-turbine, gas boiler, electric and adsorption chiller, and thermal storage units. The multi-objective function integrated 3 objectives with weight methods, which are minimizing the annual costs (including capital cost, fuel costs and grid purchase minus grid sales), minimizing CO2 emissions from both grid and natural gas combustion, and minimization of primary energy consumption. Zeng et al. (2020) simulated traditional electrical and thermal load following dispatch strategies as well as improved strategies. Optimality was achieved with the improved thermal load following which utilized full solar PV power output, and the surplus waste heat (exceeding the demand) is used to supply the chiller to cover the cooling demand which occurs in the same time, and this might not be realistic but not explained in the paper. It is noted that energy is purchased from the grid contributed by more than 50% and due to the absence of profit estimation, it is not clear how this high share of the grid is beneficial. In addition, efficiencies are taken as constants to linearize the optimization. Previously explained studies' findings and other relevant studies with their key considerations are summarized in Table 1.

2.2. Regulated market

The minimization of COE is disregarding profit from trading with the grid and lack a proper modeling of an hourly simulation of VPPs. Related studies aimed to find optimal (minimum) sizes of power plants and found the required COE (i.e. Electricity tariff) to be collected by power plants to break-even, without actual consideration of the feasibility of this COE in their markets. As an example, Diab et al. (2019) evaluated different meta-heuristic optimization methods (Whale Optimization, Water Cycle, Salp Swarm and Grey-Wolf algorithms) to schedule an on-grid hybrid system of solar-wind-pumped-hydro storage power plant near Ataka region east of Egypt. Results showed that the Whale Optimization Algorithm (WOA) yielded the optimum Cost of Energy at 0.217 $/kWh (3.38 EGP/kWh), which is higher than the current electricity tariff in Egypt as mentioned before. Similarly, Barakat et al. (2016) took advantage of the newly introduced feed-in tariff in Egypt and attempted to estimate the size and number of modules of a grid-connected hybrid system consisting of several units of 1 kW solar PV unit, 10 kW wind turbine, 50 kW biogas-power plants and 100 kW battery, aiming to minimize the Net Present Cost (NPC). Optimization is solved with HOMER, and the optimal system showed a solar and wind power share of 24.4% and 42.7% respectively. However, the study also did not consider any market constraint and presented a hypothetical model without exploring the actual market condition.

An off-grid model was presented in Elkadeem et al. (2020) also aiming to find the sizes of the hybrid system components (wind turbine, solar PV, diesel generator, fuel cell, batteries, and gas-fired boiler) that would achieve the minimum cost of energy (which involves the investment costs). The model is solved with HOMER and achieved 0.15 $/kWh (2.34 EGP/kWh) 17.2 kW for solar PV, 5 kW Fuel cell, one 10 kW Wind Turbine, 70 battery units (each having 914.3 kWh capacity), which is higher than electricity tariff. In Elkadeem et al. (2020) the energy exchange with the grid was not considered, although the system produced a surplus of 24,738 kWh/year, also the amount of utilized waste heat from the fuel cell while covering thermal load was not analyzed in term of how this waste would affect the overall efficiency and emissions from the system.

El-Sattar et al. (2021) used Tunicate Swarm Algorithm (TSA) to estimate the size and configuration of a Microgrid by minimizing the COE. The Microgrid is in islanded mode and consists of solar PVs, wind turbines, battery storage and a diesel generator. The achieved COE is 0.33 $/kWh, which is higher than the electricity tariff. The study disregarded the ability to interact with the grid and the revenues coming from trading electricity. Attempting to explore more algorithms, El-Sattar et al. (2021) compared in another study 4 different optimization algorithms, namely Slime Mould Algorithm (SMA), Seagull optimization algorithm (SOA), gray Wolf Optimizer (GWO), Whale Optimization Algorithm (WOA), and Sine Cosine Algorithm (SCA), to find the optimal configuration of a hybrid system to minimize the COE. The study aggregated solar PV, Wind turbines, biomass generator and battery system, and achieved a COE of 0.11 $/kWh with SMA, although this COE is higher than the electricity tariff.

Other studies followed the same minimum COE approach to estimate the configuration of their hybrid systems in different countries adopting regulated markets such as KSA (Ramli, et al., 2018), Ecuador (Cano, et al., 2020) and Bangladesh (Mandal, et al., 2018).

The review of previous studies revealed knowledge gaps in consideration of profit from selling energy to either the grid or to consumers. Almost all relevant studies approached the design of hybrid systems (Microgrids and VPPs) by minimization of COE which asks the customer to pay this COE for the plant to pay-off. COE values resulting from different studies varies according to location and selection of the aggregated power plants technologies. In-depth literature review revealed considerable knowledge gaps in term of new method:

1- The formulation of profit maximization as an objective function to drive VPPs in real-time following energy demand profiles
2- Consideration of realistic market boundaries and incentives that bind the energy trading of VPPs (or aggregated DERs in general term), such as PPA in the context of this study.
3- Modeling simultaneous power and thermal energy trading between VPPs stakeholders (consumers, grid and power plants) and reflection of this profit outcome in optimization objective function

This work seeks to advance the state of the art and address the knowledge gaps. The main contribution of the paper could be summarized as follow:

1- To our knowledge, this work is the first to present an hourly demand data-driven optimization for VPPs in regulated markets with profit maximization as a novel objective function for this specific market category.
2- This work will be the first to consider VPPs with non-linear part-load efficiency consideration . For that reason, GA will be employed to solve the optimization problem being efficient in solving non-linear objective functions and constraints.
3- Finally, to the best of knowledge, this work is the first to propose, in regulated market cases, a simultaneous power and thermal energy trading considering energy sales incoming from selling power to grid and to consumers, and from selling thermal energy to consumers. This framework aims to enhance the flexibility of operation of the overall system, energy efficiency and profitability of VPPs.

The proposed method is tested in Egypt as a case study considering the existing market prices and electricity tariffs. However, regardless of the case study location, the framework and formulation of objective function, considering profit through energy sales, is applicable to all similar regulated markets where government owned-utilities control the power distribution.

The rest of the paper is organized as follows: Section 2 illustrates the conceptual framework of the proposed VPP system, simulation scenarios (configurations) and optimization solution method, Section 3 presents the VPP components modeling and optimization problem formulation, Section 4 presents the case study data and results, Section 5 presents the results summary and analysis, and finally Section 6 presents the conclusion.

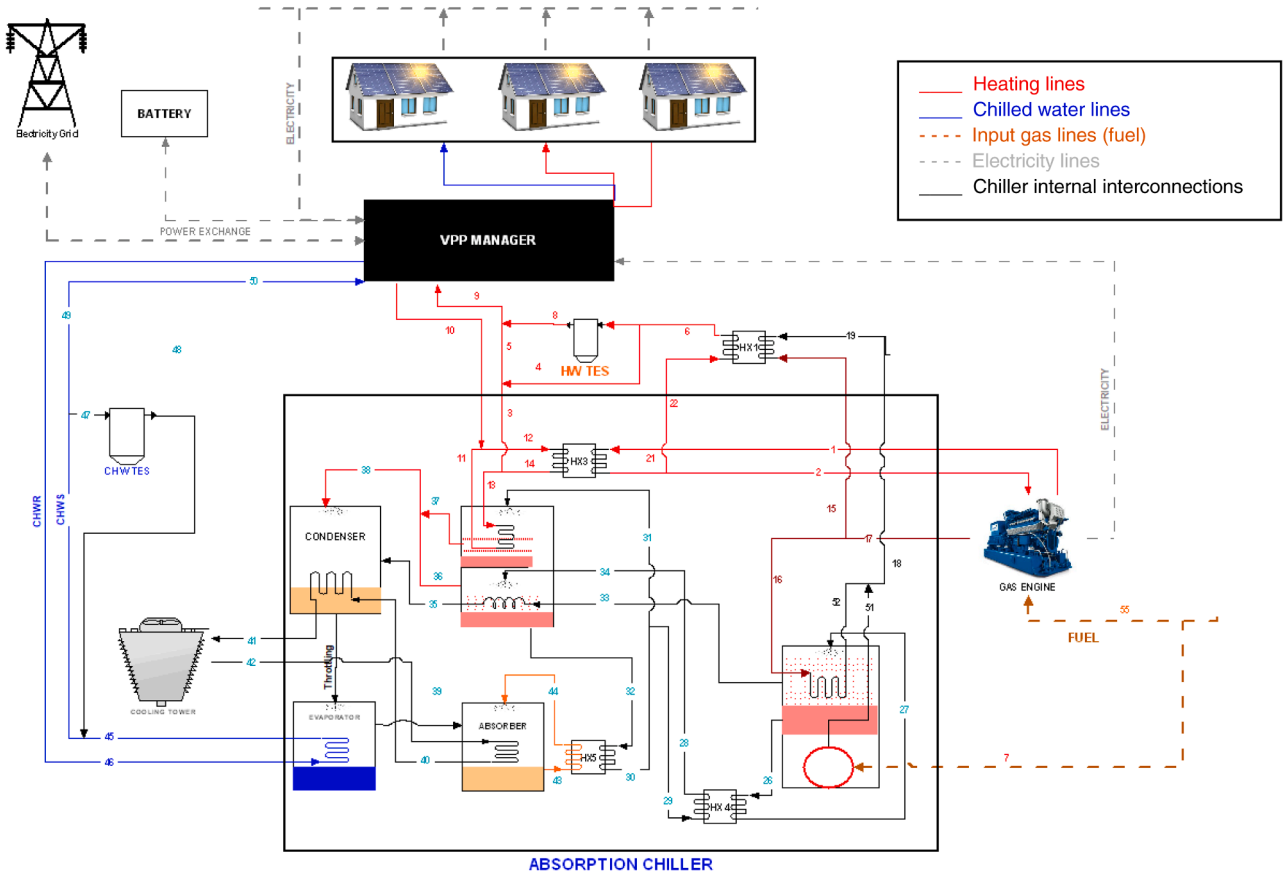

Fig. 1. VPP System and components diagram.

3. Methodology

3.1. Concept description

The objective function will be formulated to maximize the profit, considering a common approach adopted in most regulated countries which is power purchase agreements (PPA). In this research, the case study will be implemented in Egypt, which recently allowed private investors to implement the IPP policy to initiate more solar and wind power generation projects to be sold to the grid under PPA, with an agreed tariff set by the government. This tariff was set at 0.38 EGP/kWh (0.025 $/kWh) as a maximum price for bidders during initiation of a project back in 2019 (Bellini, 2019), which is slightly lower than the LCOE of solar PV (0.03 $/kWh) (NREL, 2021). Until today, there has been no clear regulation for IPP projects for conventional or biomass thermal power plants to exchange energy with the grid, the market reform was mainly incentivized for the sake of solar and wind power. Rooftop Solar PV could be installed by household owners or by the residential project developers, to reduce the dependency on the electricity from the grid, with the opportunity to explore the IPP incentives for solar PV and without the need for a large area for a central solar PV plant. However, due to their stochastic nature and uncertainty in power generation, solar power operation management is improved where thermal power plants (e.g., diesel generators, gas engines, biomass plant) are associated (Ko & Kim, 2019).

The proposed energy system is assumed to be owned by the residential compound project developer. The VPP is a central aggregator that manages the supply of power, heating, and cooling energy, and controls the exchange of power from and to the grid, as illustrated in Fig. 1. The aggregated system is composed of a natural gas-fired CCHP, double effect direct-fired absorption chiller, hot water storage, and ice storage systems, rooftop solar PV panels, and Battery Storage System (BSS). As this research focuses on low- and middle-income residential communities around Cairo, their buildings are mostly characterized

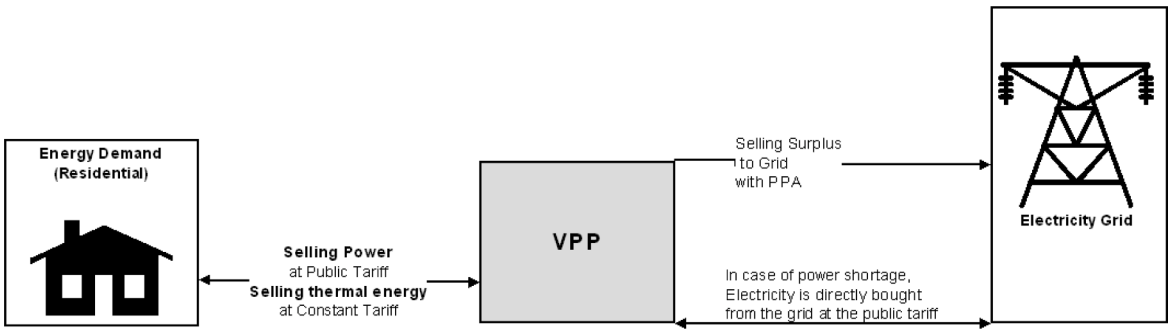

Fig. 2. VPP Energy trading conceptual diagram.

Table 2
Simulation scenarios summary.

	Scenario 1	Scenario 2	Scenario 3	Scenario 4	Scenario 5
CCHP Operation Strategy	Hybrid power/thermal load following	Hybrid power/thermal load following	Thermal load following	Hybrid power/thermal load following	-
Max. Profit	✔	✔	-	✔	✔
Max. Energy & Exergy Efficiency	-	-	✔	-	-
CCHP	✔	✔	✔	✔	-
Double Effect AC	✔	-	-	✔	-
Double Effect AC + Direct Firing	-	✔	-	-	-
TES	✔	✔	-	-	-
BSS	✔	✔	-	-	-

with flat roofs, 6 floors, each contains 4 × 80–90 m^2 apartment. It is assumed that 60% of the roof can be utilized for solar PV panels installation (Paidipati, et al., 2008).

The heating and cooling demand are covered by district energy replacing the air conditioners that are used to cover the space cooling and heating requirements. The heating and cooling load covered by air conditioners is converted to the electrical load and subtracted from the total power demand since it is covered by another source. The district energy is sold to customers at an assumed price equivalent to solar PV PPA price. The net power demand (minus cooling and heating load) is supplied by the VPP and the consumer is charged the normal public energy tariff. Thermal storages and BSS are attached to the VPP to store the surplus and discharge at shortage or peak periods; however, this operation philosophy of storage systems would vary in this study as per the dispatch decision from the optimization. In markets where energy prices are variable with time, storage systems are used to perform arbitrage and make profits such as the case in Nezamabadi & Nazar (2015).

Therefore, the model assumptions and conceptual framework be summarized as follows as illustrated in Fig. 2:

- The VPP aggregates solar PV units, CCHP, BSS and Thermal storage system
- The VPP sells surplus power to the grid as a PPA agreement ("pay as generated" concept)
- The VPP sells power to residential consumers at the Public electricity tariff, and sells thermal energy at a constant tariff equivalent to the same PPA price of solar power sales to the grid
- Solar PVs are assumed to occupy all roofs
- In case of power shortage, VPP purchases electricity from the grid and supply it to consumers without profit

3.2. Public Electricity tariff definition

In the Egyptian market, the tariff is flat with time is sliced for each range of energy consumption (kWh), the consumer is charged equivalent to his monthly consumption (kWh) x Tariff for the slice of his consumption. The consumer is charged 0.38 EGP/kWh for 0-50 kWh consumption, 0.48 EGP/kWh for 51-100 kWh, 0.65 EGP/kWh for 100-200 kWh, 0.96 EGP/kWh for 201-350 kWh, 1.28 EGP/kWh for 351-650 kWh and 1.45 EGP/kWh for more than 1000 kWh monthly consumption (Egypt Independent, 2021). For simplification, the maximum price of the last slice is used in this study, which is 1.45 EGP/kWh (0.092 $/kWh) (Egypt Independent, 2021). As prices are flat with time, the storage systems would not perform arbitrage and their economic viability, in this case, are questionable. For sizing purposes and for a deeper understanding of the relations between components, multiple iterations are performed to simulate the overall results of different CCHP sizes, in order to draw statistical relations between the plant capacity, solar power penetration ratio, VPP profit, and overall energy and exergy efficiency.

3.3. Energy balance

The operation strategy of CCHPs is usually based on following the heat demand (Wang, et al., 2011) or following the electricity demand (Liu, et al., 2013). Each strategy has its drawback in case the plant is allowed to exchange power with the grid; following heat demand results of the forced reduction of power output and accordingly produces lower surplus than its potential meaning less profit, on the other hand, following power demand would produce a surplus heat and will be dumped to the atmosphere to maintain the cooling and heating supply and demand balance. In this study, either maximizing the VPP profit and maximizing its efficiency and exergy will be studied, the mean of the amount dumped heat will be evaluated in both cases.

3.4. Simulation scenarios

Multiple scenarios are simulated by changing the configurations of the hybrid system, to extract statistical relations between the CCHP and solar PV power capacities, efficiency, exergy, and amount of dumped heat. These relations will be applicable for similar residential cases by providing developers and decision-makers insights and a better understanding of the tradeoff between the performance (exergy and energy efficiency) and the achieved profits, which enables proper decision making for both operation management and design planning of hybrid plants. AC is initially assumed as double effect and direct-fired, to allow flexible and decoupled operation between heat and power, however, the direct-firing option must be evaluated to decide its viability. As can be noted, there would be lot of scenarios to simulate different configurations and sizes. Most notable scenarios are reported in this study, where the main variables between these scenarios are AC direct firing option (using natural gas as input along with waste heat), Storage units' inclusion and objective functions evaluation Eqs. (1) and ((2)).

The first 2 scenarios will evaluate the economic objective function with and without the AC direct firing. Whichever option proved more profitability will be used in the further scenarios. Scenario 3 will evaluate the performance objective function using thermal load following strategy. Scenario 4 will evaluate the system similar to scenario 1 but without thermal storage nor BSS nor AC direct firing, which is necessary to decide whether storage is profitable in the case of grid power exchange enabling. Scenario 5 will evaluate a pure solar PV with BSS, to be economically evaluated to estimate whether this system could achieve net profits or only contribute to reducing dependency on the grid power. Reported scenarios of this study are summarized in Table 2.

3.5. Optimization method

CCHP part-load efficiency is a non-linear function, and it would be necessary to consider this non-linearity for accurate fuel consumption calculation. In the literature, it was proved that the non-linearity or part-load consideration in modelling produces more advantageous results compared to linearized models (Green & Garimella, 2021) (Kamel, et al.,

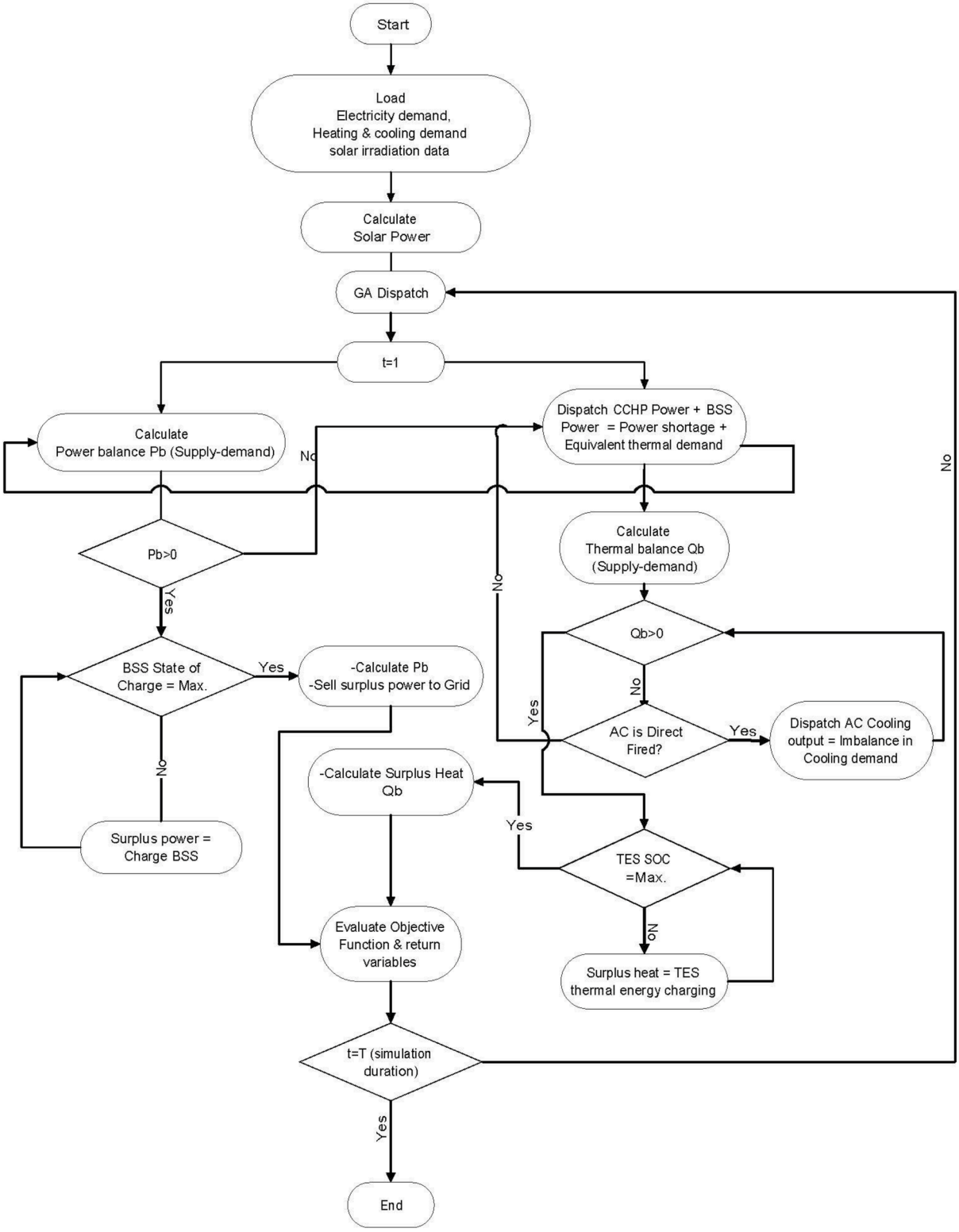

Fig. 3. VPP operation management flowchart.

2021). In addition, power dispatch requires integer binaries representing ON/OFF conditions, which turns the optimization problem to a mixed integer non-linear programming. One of the efficient category of algorithms to solve mixed integer non-linear programming is the meta-heuristic methods such as Genetic algorithms (GA), Particle swarm optimization (PSO), artificial bee colony (ABC) and simulated annealing (SA) (Mohammadi, et al., 2014). Meta-heuristic algorithms are widely used in literature to solve such complex problems, algorithms such as GA, PSO (Hadayeghparast, et al., 2019), Ant colony (Abo-Elyousr & Elnozahy, 2018), Imperial Competitive algorithm (Kasaei, et al., 2017), and others. By comparing the most common heuristic algorithms PSO and GA, it was found that GA achieved better results than others (Maleki, et al., 2017).

In this study, GA will be employed to solve the optimization, being an

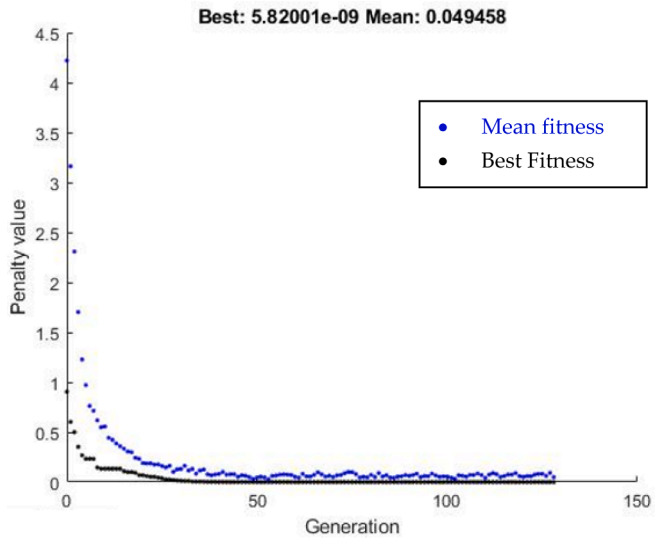

Fig. 4. GA Evolution diagram.

efficient algorithm to handle complex problems with non-linear as well as mixed integers without getting restricted to local optima (Koutroulis, et al., 2006). Operation management framework of the integrated systems with GA is illustrated in Fig. 3. Although it is deemed a suitable option for solving complex problems with large searching space (Tabassum & Mathew, 2014), it will be insightful to compare optimal configuration achieved by GA in this study against solutions with other optimization algorithms to help refining the results. Such a comparison is beyond the scope of this study and will be considered as a further work. GAs intend to initialize a population of chromosomes (Population Size) representing combination sets of optimization variables whose values are defined with a random function, those are initial candidate solutions to the optimization. Each set of chromosomes are tested against a fitness value (objective function), whichever achieved the lowest fitness value are selected to form new chromosomes in the new generation, those are called elite, and their count should be defined (Elite Count). New chromosomes created by Elite sets in the new generation are formed through "Crossover" and "Mutation" operators. "Crossover" operator reorganizes 2 different sets of chromosomes (parents) to create a new set (children) sharing information (genes) from both parents, while "Mutation" operator randomly changes the values of each new set according to mutation probability, this is essential to avoid early convergence of the solver (Herrera & Magdalena, 1997) (Deb, 2001) (Mondal, et al., 2020) . Due to the possible randomness nature of the solver, GA could yield a different set of solutions at each run. To find the optimal configuration, multiple iterations were performed, and the following parameters were found suitable to stabilize the solution.

- Population Size= 150
- Number of Generations = 150
- Elite count = 10
- Fitness Function tolerance = 1 × 10^-8
- Constraint tolerance = 1 × 10^-8
- Crossover fraction = 0.8

From the initial iterations, convergence of the model is checked, as shown in Fig. 4, by plotting penalty value against the evolved generations (done in each time step) and a low mean value close to zero is verified.

4. VPP Model

As described in Section 2, the VPP aggregated a CCHP, solar PVs, AC, TES and BSS units. Modeling and energy balance of the overall system, and selection of CCHP type are described in the following subsections.

4.1. CCHP

As shown in Table 3, both reciprocating engine and gas turbine technologies have a low start-up time which is necessary when needed to respond quickly to intermittent power. Steam turbines although having the minimum capital cost per MW among other technologies, have a relatively long start-up time (Moussawi, et al., 2017). Part-load, which is a major consideration in this study, is affecting the overall efficiency of the plant. However, as solar power is part of the aggregated power and thermal supply of the system, the engine's ability to operate at part-load is essential for maintaining efficiency. All technologies are supposed to operate at full load and sometimes at part-load but at part-load efficiency decreases. Many studies on aggregated power plants ignored the efficiency variation with part load and assumed constant efficiency for simplification (Alipour, et al., 2014) (Kasaei, et al., 2017) (Maleki, et al., 2017), this can reduce the accuracy of results and could mislead the decision on plant sizing.

Reciprocating engine (Spark ignition) shall be used in this study with generic variable efficiency data. Typical power to heat ratio falls in the range of 0.5–1.2 (Darrow, et al., 2017), for simplification of the optimization algorithm, this ratio is assumed as 1. The main sources of heat which could be significantly recovered from ICE engines is a low-grade heat from jacket water served to cool the engine, and high-grade heat from exhaust in the combustion process (Zhoua, et al., 2013). The jacket water can reach a temperature of 90°C, while exhaust gas fluctuates between 400–600°C (Wang & Wu, 2015). For the sake of utilizing both heat sources, a double-effect absorption chiller will be used to provide chilled water output at the range of (7–12 °C). An overview of the types of absorption chiller shall be discussed in the next section.

4.2. Absorption chillers

The most common type of absorption chillers is LiBr-H2O, divided to two types: single effect which recovers temperatures less than 120°C with a typical COP of around 0.7, and double effect which recovers exhaust heat and temperatures more than 120°C with a typical COP of around 1.4 (Deng, et al., 2011). By combining the single and double effect cycles, a mixed effect absorption chiller is introduced to recover

Table 3
Comparison between CCHPs prime movers' parameters (Moussawi, et al., 2017).

Prime mover technology	Steam Turbine	Gas Turbine	Micro Turbine (small gas turbines ranging between 30-350 kW)	Internal Combustion Engine (Spark Ignition)
Power to heat ratio	0.05-0.2	0.5-2	0.4-0.7	0.5-1
Capital Cost ($/kW)	200-1000	400–1800	1300–2500	900–1500
Maintenance Cost ($/kWh)	<0.002	0.003–0.01	<0.018	0.007–0.02
Start-up time	Hours	Minutes	Minutes	Seconds
Part load performance	Good	Poor	Fair	Good
CO2 emissions (kg/MWh)	Variable as per steam source	580-680	720	500-620

both low-temperature jacket cooling water and high-temperature exhaust heat. Many studies employed direct-fired absorption chillers (associating the mixed effect chiller) which use natural gas as a fuel to create the input high-grade heat when there is no enough waste heat from the prime mover to cover the heating or cooling demand (Wang, et al., 2015) (M.I. Alhamid, et al., 2020) (Wang, et al., 2016). In this research, a mixed type AC having COP=1.4, will be tested with and without the direct firing capability to evaluate its impact on the overall performance of the CCHP.

4.3. Solar PV

Solar PV output power is converted from solar irradiation at the location of the case study, assumed available rooftop area and PV panel efficiency. Conversion efficiency depends on the panel temperature which depends on the ambient temperature; therefore, it is variable with time, and this is taken into consideration in the model. Data for ambient and solar irradiation is obtained from PV GIS online tool (EU Science Hub, 2019) for the specified case study location.

4.4. BSS & TES

Batteries are used to store surplus electrical energy to be used when there is more demand. Specifically, in the case of solar power, it stores excess energy in the morning and discharges it at night where the demand is at its peak. However, in this study, it is assumed that the direct utilization of energy is more economically efficient than storing, this would be only possible in the case of possible energy exchange with the grid and availability of another power source, such as the CCHP in this case. This assumption shall be validated by simulating cases with and without batteries and estimating the profit for both cases. Thermal storages are also employed to store hot water or chilled water for later utilization. Roundtrip efficiency for each of BSS and TES systems is assumed as 90%.

4.5. Model formulation

The proposed model is selling energy directly to customers and exchanging with the grid in the following strategies:

- In case of shortage than the power demand: the VPP purchases energy from the grid and supplies it to the consumer at the public energy tariff, without achieving any profit.
- In case of surplus than the power demand: the VPP sells energy to the grid as a PPA contract, at the minimum PPA price announced by the government for Solar PV projects (Bellini, 2019).

Two objective functions are evaluated separately, the first one aims to maximize the VPP profit and tailored as per the 2 selling stages to consumers and to the grid. The second objective function aims to maximize both energy and exergy efficiency using the equal weigh multi-objective method. It has been proven in the literature that equal weight produces as good results as the optimal weighing method produces (Zeng, et al., 2016). With both objective functions, multiple iterations using different configurations, as described in the scenarios, will be performed to minimize dumped heat.

The GA is implemented to search for the values of the decision variables to satisfy the objective functions. The decision variables of the optimization are the CCHP output power, absorption chiller's input fuel flow rate, charging/discharging power of the BSS, stored thermal energy charging/discharging, heating/chilled water output temperature, exchanged power with the grid and binaries to control the ON/OFF statuses of CCHP, thermal storage, BSS and Sold/Purchased energy to/from the grid, to help reduce the randomness of the algorithm.

The first objective function is stated as follows:

$$\sum_{t=1}^{T} Profit = \sum_{t=1}^{T} \left(P_{CCHP,\,t} + P_{PV,\,t} + u_{BSS-disch,t}.P_{disch,t} - P_{gridsell,t}\,.\,\left(1-u_{grid,t}\right) - P_{gridbuy,t}\,.\,u_{grid,t}\right)\,.\,\lambda_{el,\,t} + \left(P_{gridsell,t}\,.\,\left(1-u_{grid,t}\right)\right)\,.\,\lambda_{PPA,\,t} + \left(Q_{CHW\_demand,t} + Q_{HW\_demand,t}\right)\,.\,\lambda_{DE,\,t} - \left(\left(\dot{m}_{f,t}+\dot{m}_{f-ac,t}\right).C_f + C_{SU}.SU_t + \left(u_{CHW-ch}\,.\,Q_{CHW-TS-charge,t} + u_{HW-ch}\,.\,Q_{HW-TS-charge,t}\right).C_{ch,t}\right) \quad (1)$$

The above equation describes the profit from selling energy in the following stages:

A- Selling power to consumers equivalent to their electricity demand at $\lambda_{el,\,t}$ price (standard electricity tariff); therefore ($P_{CCHP,\,t} + P_{PV,\,t} + u_{BSS-disch,t}.P_{disch,t} - P_{gridsell,t}\,.\,u_{gridsell,t}$) is the output power from CCHP + solar PV + discharged BSS power excluding any surplus that exceeds the electricity demand. $P_{gridsell,t}\,.\,u_{gridsell,t}$ is subtracted to prevent any surplus to be sold at the electricity tariff. $P_{gridbuy,t}\,.\,u_{gridbuy,t}$ is also subtracted because when the VPP has a shortage, power is purchased from the grid and sold to consumers directly without profit.

B- Selling the surplus at $\lambda_{PPA,\,t}$ (PPA price); + $\left(P_{gridsell,t}\,.\,u_{gridsell,t}\right)\,.\,\lambda_{PPA,\,t}$

C- Selling the thermal energy to consumers at $\lambda_{DE,\,t}$ (District energy tariff); $\left(Q_{CHW\_demand,t} + Q_{HW\_demand,t}\right)\,.\,\lambda_{DE,\,t}$

The second objective function is stated as follows (Wang, et al., 2016):

Maximize:

$$\sum_{t=1}^{T} Performance = \sum_{t=1}^{T} (\omega 1\,.\,Energy\_Efficiency_t + \omega 2\,.\,Exergy\_Efficiency_t) \quad (2)$$

$$\omega 1, \omega 2 = 0.5 \quad (3)$$

$$Energy\_Efficiency_{\,t} = \frac{P_{CCHP,\,t} + \left(Q_{CHW,t} + Q_{CHW-ac,t}\right)/COPc + Q_{HW,t}}{\dot{m}_{f,t}.LHV_f + \dot{m}_{f-ac,t}.LHV_f} \quad (4)$$

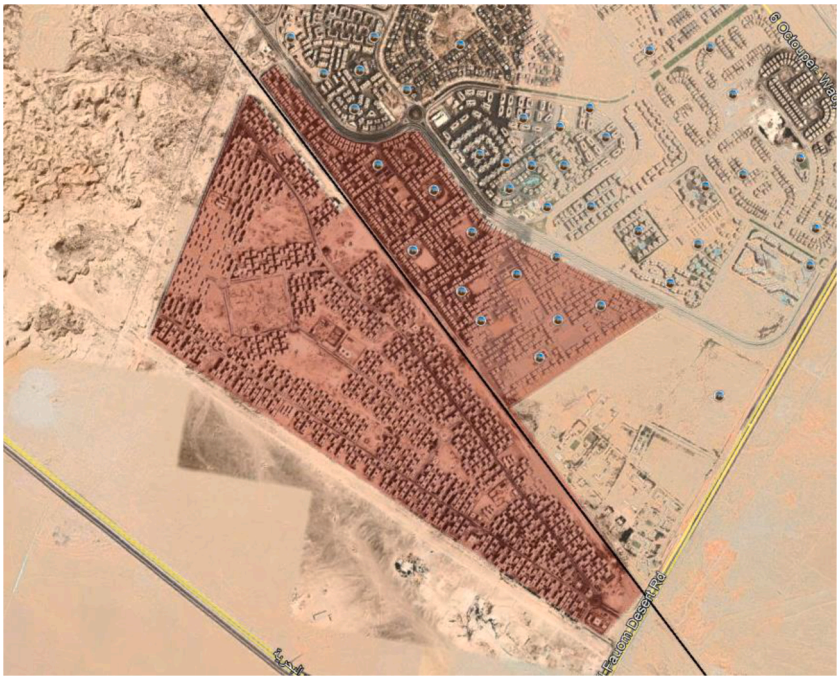

Fig. 5. Case Study boundaries (Google Earth, 2020).

$$Exergy\_Efficiency_{\ t} = \frac{P_{CCHP,\ t} + \left(\left(Q_{CHW,t} + Q_{CHW-ac,t}\right)/COPc\right) \cdot \left(\frac{T_{o,\ t}}{T_{CHW,t}} - 1\right) + Q_{HW,t} \cdot \left(1 - \frac{T_{o,\ t}}{T_{HW,t}}\right)}{\dot{m}_{f,t}.HHV_f + \dot{m}_{f-ac,t}.HHV_f} \tag{5}$$

Subjected to (Constraints):

$$SU_t = v_t(1 - v_{t-1});\ t = 1,\ \ldots,\ T \tag{6}$$

$$v_t \in \{0,1\};\ t = 1,\ \ldots,\ T \tag{7}$$

$$u_{grid} \in \{0,1\};\ t = 1,\ \ldots,\ T \tag{8}$$

$$u_{cchp}\ x\ P_{CCHP_{min}} \le P_{CCHP,\ t} \le u_{cchp}\ x\ P_{CCHP_{max}};\ t = 1,\ \ldots,\ T \tag{9}$$

$$323\ ^{\circ}\mathrm{K} \le \mathrm{T_{HW,t}} \le 343\ ^{\circ}\mathrm{K} \tag{10}$$

$$278\ ^{\circ}\mathrm{K} \le \mathrm{T_{CHW,t}} \le 280\ ^{\circ}\mathrm{K} \tag{11}$$

$$0 < P_{gridbuy,t} < P_{gridbuy\_max,t} \tag{12}$$

$$0 < P_{gridbuy,t} < P_{gridbuy\_min,t} \tag{13}$$

State of Charge for TES and BSS is estimated as follow (Ren, et al., 2008):

$$E_{CHW-TS,t} = (1 - \varepsilon_t).E_{CHW-TS,t-1} + u_{CHW-ch} \cdot Q_{CHW-TS-ch,t} - u_{CHW-ch} \cdot Q_{CHW-TS-disch,t} \le E_{CHW-TS\_max,t};\ t = 1,\ \ldots,\ T \tag{14}$$

$$E_{HW-TS,t} = (1 - \varepsilon_t).E_{HW-TS,t-1} + u_{HW-ch} \cdot Q_{HW-TS-ch,t} - u_{HW-disch} \cdot Q_{HW-TS-disch,t} \le E_{HW-TS\_max,t};\ t = 1,\ \ldots,\ T \tag{15}$$

$$E_{BSS,t} = E_{BSS,t-1} + u_{BSS-ch}\eta_{charge}P_{charge,t-1} - u_{BSS-disch}\left(\frac{1}{\eta_{discharge}}\right)P_{disch,t-1} \le E_{BSS\_max,t};\ t = 1,\ \ldots,\ T \tag{16}$$

$$u_{CHW-ch} + u_{CHW-disch} \le 1;\ u_{CHW-ch}, u_{CHW-disch}\ \epsilon\ \{0,1\} \tag{17}$$

$$u_{HW-ch} + u_{HW-disch} \le 1;\ u_{HW-ch},\ u_{HW-disch}\ \epsilon\ \{0,1\} \tag{18}$$

$$u_{BSS-ch,t} + u_{BSS-disch,t} \le 1;\ u_{HW-ch},\ u_{HW-disch}\ \epsilon\ \{0,1\} \tag{19}$$

Output from Solar power and PV panel efficiency are estimated as follow (Kolhe, et al., 2003):

$$P_{PV,\ t} = \eta_{PV}A_{PV}G_t;\ t = 1,\ \ldots,\ T \tag{20}$$

$$T_{c,t} = T_{o,t} + \left[\left(\frac{NOCT - 20}{800}\right)\right] \cdot G_t;\ t = 1,\ \ldots,\ T \tag{21}$$

$$\eta_{PV} = \eta_r\ x\ \left[1 - \beta\left(T_{c,t} - T_{ref}\right)\right];\ t = 1,\ \ldots,\ T \tag{22}$$

Power and thermal demand balance constraints are estimated as follow:

$$COP_c.\left(\gamma \cdot P_{CCHP,\ t} + \dot{m}_{f-ac,t} \cdot LHV_f\right) + \eta_{TES} \cdot u_{CHW-disch} \cdot Q_{CHW-TS-discharge,t} - \eta_{TES} \cdot u_{CHW-ch} \cdot Q_{CHW-TS-charge,t} \ge Q_{CHW-demand,t};\ t = 1,\ \ldots,\ T \tag{23}$$

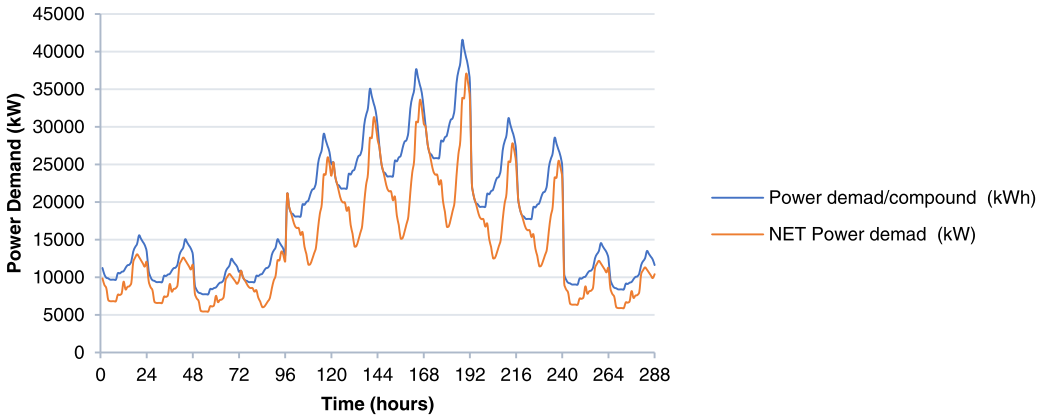

Fig. 6. Power demand profile. Net Power demand is excluding the cooling and heating load.

$$COP_c.\left(\gamma\ .\ P_{CCHP,\ t} + \dot{m}_{f-ac,t}\ .\ LHV_f\right) + \eta_{TES}\ .u_{CHW-disch}\ .\ Q_{CHW-TS-discharge,t} - \eta_{TES}\ .\ u_{CHW-ch}\ .\ Q_{CHW-TS-charge,t} \geq Q_{CHW-demand,t}; t = 1,\ \ldots,\ T \tag{24}$$

$$COP_h\ \left(\gamma\ P_{CCHP,\ t}\right) + \eta_{TES}\ .u_{HW-disch}.Q_{HW-TS-discharge,t} - \eta_{TES}.u_{HW-ch}.Q_{HW-TS-charge,t} \geq Q_{HW-demand,t};\ t = 1,\ \ldots,\ T \tag{25}$$

$$Q_{recovered} = Q_{exh} + \ Q_{jw} = \gamma\ .\ Pcchp \tag{26}$$

Part-load electrical efficiency modeling of the CCHP is expressed as a function of nominal efficiency, estimated as follows (A.Kamel, et al., 2019):

$$\eta_{CCHPe\_nominal} = 0.0194\ ln(P_{CCHP_{max}}) + 0.2321 \tag{27}$$

$$\eta_{CCHPe,t} = \eta_{CCHPe\_nominal}\ (0.1024\left(\frac{P_{CCHP,t}}{P_{CCHP_{max}}}\right)^3 - 0.7332\left(\frac{P_{CCHP,t}}{P_{CCHP_{max}}}\right)^2 + 1.0155\left(\frac{P_{CCHP,t}}{P_{CCHP_{max}}}\right) + 0.6153 \tag{28}$$

$$\dot{m}_{f,t} = \frac{P_{CCHP,t}}{\eta_{CCHPe,t}.\ LHVf};\ t = 1,\ \ldots,\ T \tag{29}$$

The CO2 emissions are calculated as per the following formula (Zheng, et al., 2014):

$$F_{CO2,\ total} = 30\ x\left(\sum_{t=1}^{T}\dot{m}_{f,t}.LHV_{\ f}.\mu_{CO2_{NG}} + \sum_{t=1}^{T}\dot{m}_{f-ac,t}\ .LHV_{\ f}.\mu_{CO2_{NG}} + \sum_{t=1}^{T}P_{gridbuy,t}\ .\ \mu_{CO2_{grid}}\right) \tag{30}$$

Eq. 4 and 5 express the overall CCHP energy and exergy efficiency including the absorption chiller, the formulas are a modified version from Wang, et al., 2016), where $Q_{CHW,t}$ and $Q_{HW,t}$ were initially formulated as cooling and heating demand. However, it miscalculates the efficiencies in the case the demand is not satisfied, therefore in this study, they are formulated as the actual output energy. Constraint (6) signify that the start-up cost binary will be turned to 1 once the plant starts, and it will return to 0 in the following time step. Constraints (7), (8) are binary variables boundaries for CCHP start-up and energy purchase from the grid ON/OFF (1: Purchase; 0: Sell) respectively. Constraint (9) defines the lower and upper limits of the CCHP capacity, it is assumed that the minimum operating power of the CCHP is 30% of its nominal (maximum) capacity to preserve the electrical efficiency from significantly dropping (Arsalis, 2012) (Hermans & Delarue, 2016). Constraints (10) and (11) specified the chilled water and hot water supply temperature limits. Constraints (12) and (13) sets the lower and upper bound for energy exchanged with the grid. Constraints (14), (15) and (16) express the state of charge (SOC) of the TES and BSS. Constraints (17), (18) and (19) ensures that the charging and discharging would not occur simultaneously. Eqs. (20), ((21) and (22) formulates the solar PV power output from irradiation and panels area, cell temperature as a function of ambient temperature, and the PV panel efficiency.

Constraint (23) specified the power balance as an equality constraint since there are $P_{gridbuy,t}$ and $P_{gridsell,t}$ which serves to purchase the shortage or sell the surplus, respectively. Constraint (24) and (25) are defining the cooling and heating balance, they are examined in each objective function in 2 ways, inequality, and equality constraints. The inequality constraint allows the heating and cooling supply to exceed the demand and dump the surplus heat to the atmosphere, to follow the power output for achieving maximum profit. The equality constraint forces the CCHP to reduce its power output to follow the heating and cooling demand and minimizes the dumped heat. Eq. (26) defines the recovered heat from high-grade heat (exhaust) and low-grade heat (oil and jacket water). In this study, the heat to power ratio is assumed 1. Eq. (27) and (28) defines the part-load CCHP efficiency as a quadratic function, which is necessary to estimate the fuel flow rate (Eq. (29)) corresponding to the output power.

Total emission from the CCHP, AC and grid power for the full year can be calculated from equations (30). The following engineering parameters are considered for estimating the CO2 emissions (Wang, et al., 2011):

- CO2 emission factor from the grid μ_{CO2_grid}= 0.923 kg/kWh
- CO2 emission factor from natural gas μ_{CO2_NG} = 0.220 kg/kWh

5. Case study

The proposed VPP shall be tested on a large residential community in one of the new development projects in west of Cairo (as shown in

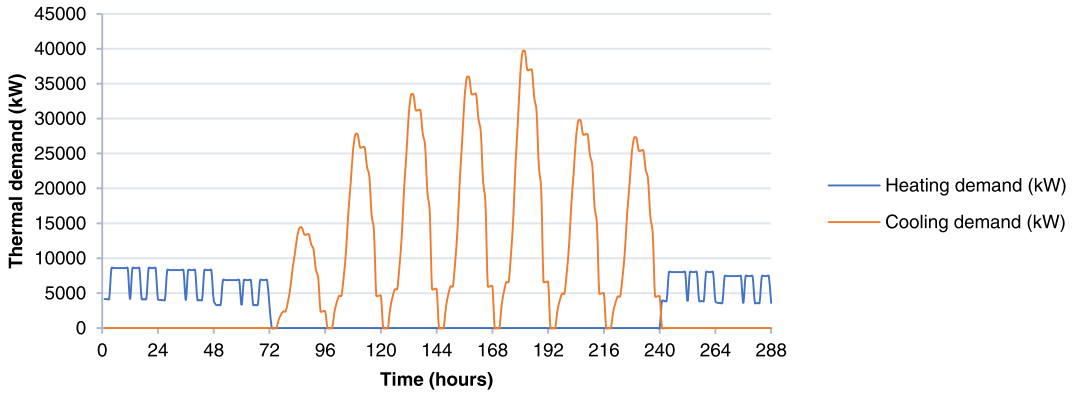

Fig. 7. Space cooling and heating demand.

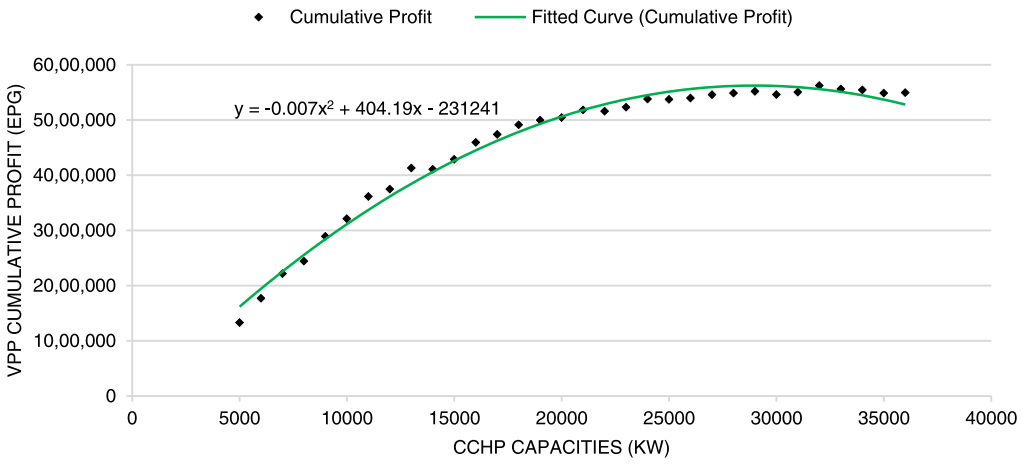

Fig. 8. VPP Profit vs CCHP Size-Scenario 1.

Fig. 5), consisting of 1185 buildings with similar shapes having flat roofs, 6 floors, each having 4 apartments of around 80 m2. The roof area is measured as 304 m2, the available area for solar PV installation is assumed as 60% of the roof area as explained before.

The estimated total available area for rooftop solar PVs is 216,144 m2. CCHP sizes are assumed to be unknown, multiple iterations shall be performed with the upper plant capacity limit is equivalent to the maximum power demand, and the algorithm will report the optimal configuration. TES units' and BSS capacities are assumed as 6 times of the CCHP and solar PV maximum capacity, with 90% efficiency. PPA price defined for energy sold to the grid is referenced from the minimum acceptable price announced by the government, which is 0.38 EGP/

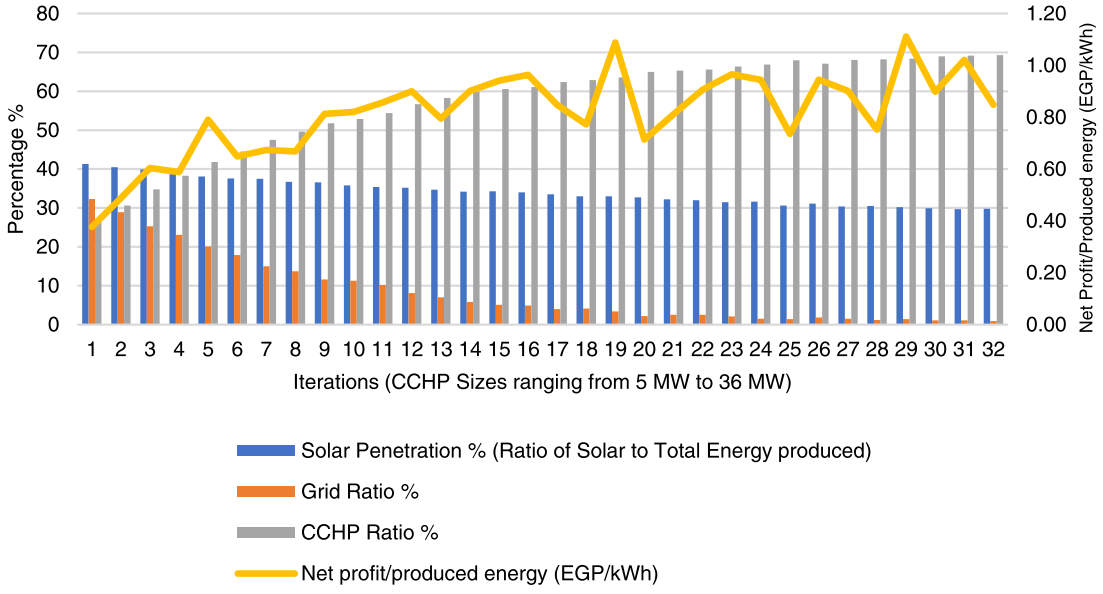

Fig. 9. Share of Power generation sources vs Profit Index-Scenario 1.

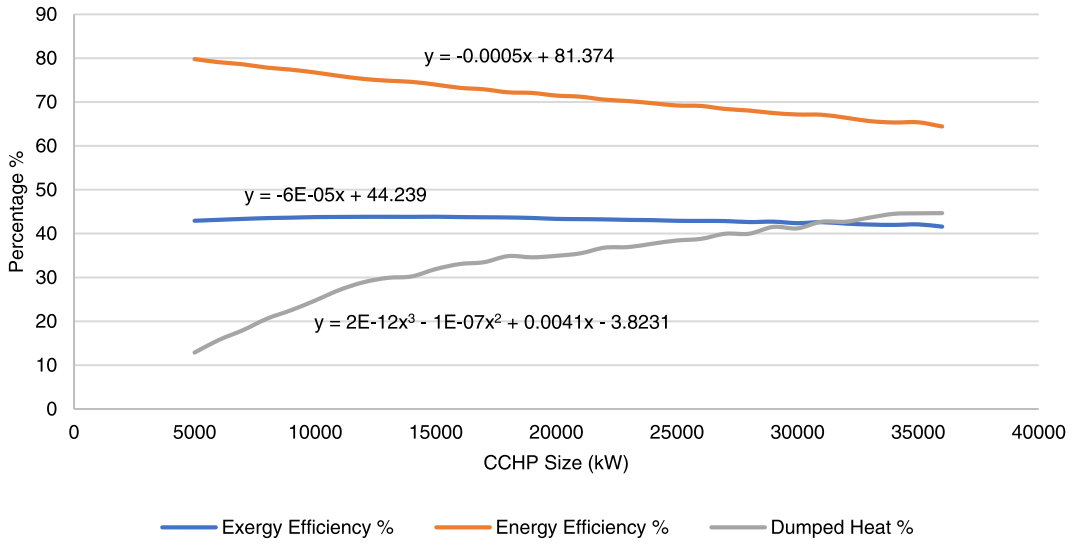

Fig. 10. Efficiencies vs Dumped heat relationship.

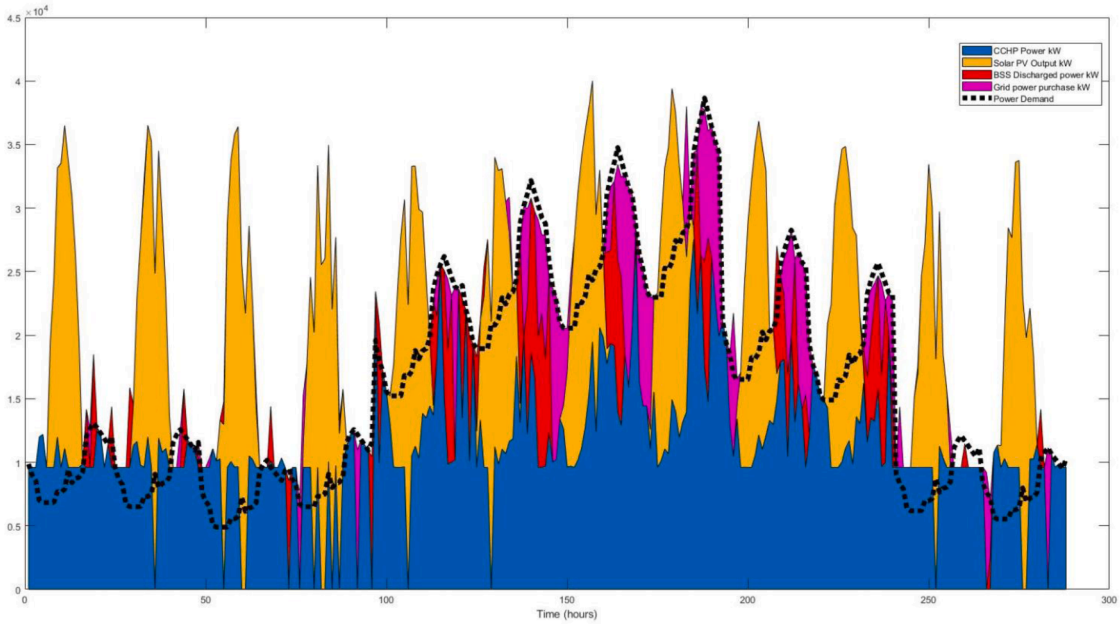

Fig. 11. Power balance-Scenario 1.

kWh, the same price is assumed as the District Energy price which is the price of cooling and heating supply to consumers. The pricing is structured so that the energy purchasing price is always higher than energy sales to the grid, which drives the optimization to minimize the energy purchase variable and aim for producing a surplus to be sold to the grid. The start-up cost is taken as 7.27 EGP/kWh (Hermans & Delarue, 2016). Absorption chiller COP is taken as 1.4 for cooling mode in summer, while in winter it acts as a heat exchanger for waste heat with an assumed efficiency of 90%. The case study is simulated over 12 days representing one day of a weekend of each month, with a resolution of 1 h, thus, 288-time steps are simulated. To evaluate the system economic, technical, and environmental viability, the proposed system will be compared with a reference case representing the traditional dependency on the electricity grid, where cooling and heating loads are covered by air conditioners. The optimization is solved with MATLAB R2020a, on a computer with an Intel® Core™ i7-9750H 2.6 GHz processor, the simulation average time is around 20 minutes.

5.1. *Energy demand data*

To optimize the strategy and resources of energy supply, the demand must be interpreted and analyzed. Due to lack of data for energy demand categorization for the residential sector in Egypt, the demand profiles are taken from the national profile (Attia, et al., 2012), normalized such that the daily average is equal to 1, and re-scaled to match the average daily power demand (Elkadeem, et al., 2020) multiplied by the appartement area. Cooling and heating are traditionally covered by Air conditioners having a COP of (3) (Hasan & Jabbar, 2021), their equivalent electricity load is assumed as 20% from the electricity demand (Aldali & Moustafa, 2016). The developed profiles are shown in Fig. 6 for electricity and Fig. 7 for space cooling and heating demand. Fig. 5 is showing the total power demand including energy needed for climate control (Air conditioners mostly), and the net power demand excluding air conditioners load. Fig. 7 is showing the actual thermal energy needed for cooling and heating. Attempts have been made in the literature to

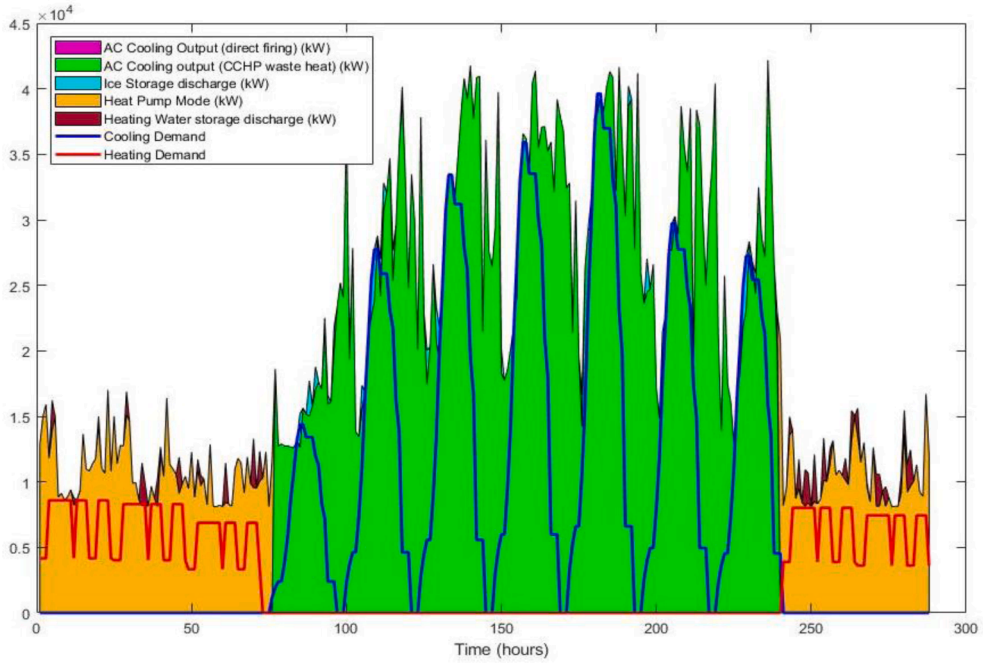

Fig. 12. Thermal balance-Scenario 1.

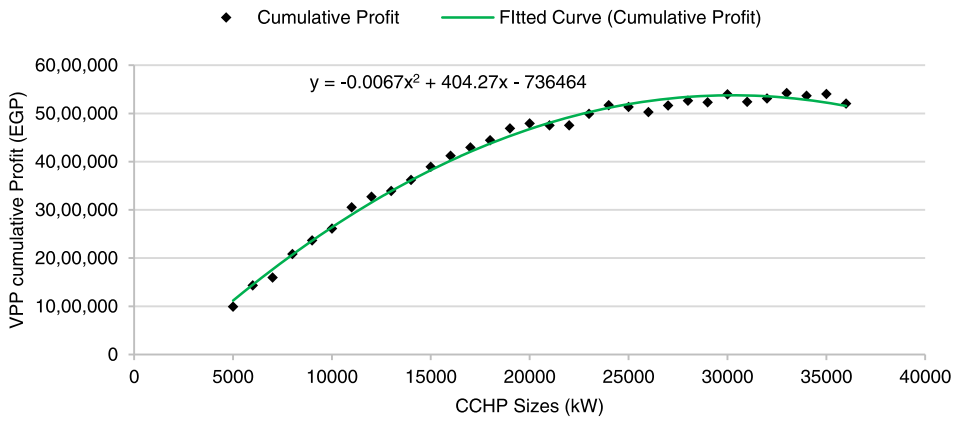

Fig. 13. VPP Profit vs CCHP peak output -Scenario 2.

estimate the demand as an average monthly value and per area, however, no hourly profiles are available for a full year, and no categorization that considers the number of occupants, their ages, installed appliances, and most importantly the hourly share of space cooling and heating load and its equivalent electrical load. Prediction of accurate energy demand profiles is not in the scope of this study and will be a further work.

5.1.1. Scenario 1: Maximizing profit, multiple CCHP sizes without AC Direct firing option

The simulation performs the hourly dispatch management for 288-time steps, iterating with multiple CCHP maximum output power generation ranging from 5 MW to 36 MW. This range is specified since that the minimum net power demand (excluding air conditioners) is around 5 MW occurring at time step 50, while the maximum is around 36 MW occurring at time step 192. So, this range 5–36 MW is assigned as initial searching space and the GA is running for multiple times considering the CCHP capacity upper bound and the program returns the size that achieves the optimal profit. In this scenario, it is assumed that the AC operates only with high- and low-grade heat output from the CCHP, without direct firing capability. The CCHP in this case is primarily driven by power demand and attempts to utilize most of the heat output, the inequality constraint for cooling and heating balance allows the waste heat to exceed the thermal demand and be dumped to generate surplus power and sell it to the grid. As prices are flat all the time, the dispatch of each plant is solely affected by the simultaneous power and thermal balance, and not by the price signals.

From Fig. 8, it can be inferred that the profit achievement is not linear with the plant capacity, and the profit almost stabilizes after 31-32 MW then it starts to reduce as the plant size increases, this is due to the increasing operational costs and the resulting surplus power that is sold back to the grid at a lower price (at the previously mentioned PPA price 0.38 EGP/kWh) than what the consumers pay (standard electricity tariff 1.45 EGP/kWh). Fig. 9 shows a normalized index for total produced energy from the proposed VPP (kWh) divided by the achieved cumulative profit, this index can represent the economic efficiency to correlate the contribution percentage of solar power, CCHP, and the purchased energy from the grid. It can be deducted that as the contribution of solar power decreases and generation from the CCHP dominates, the economic efficiency increases, controversially, as shown in

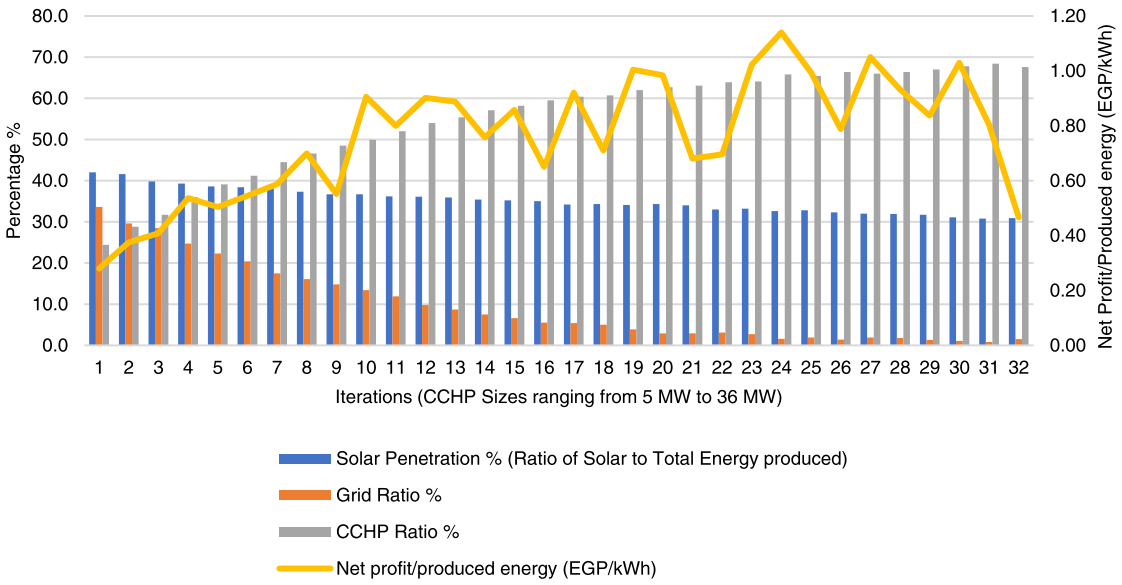

Fig. 14. Share of Power generation sources vs Profit Index-Scenario 2.

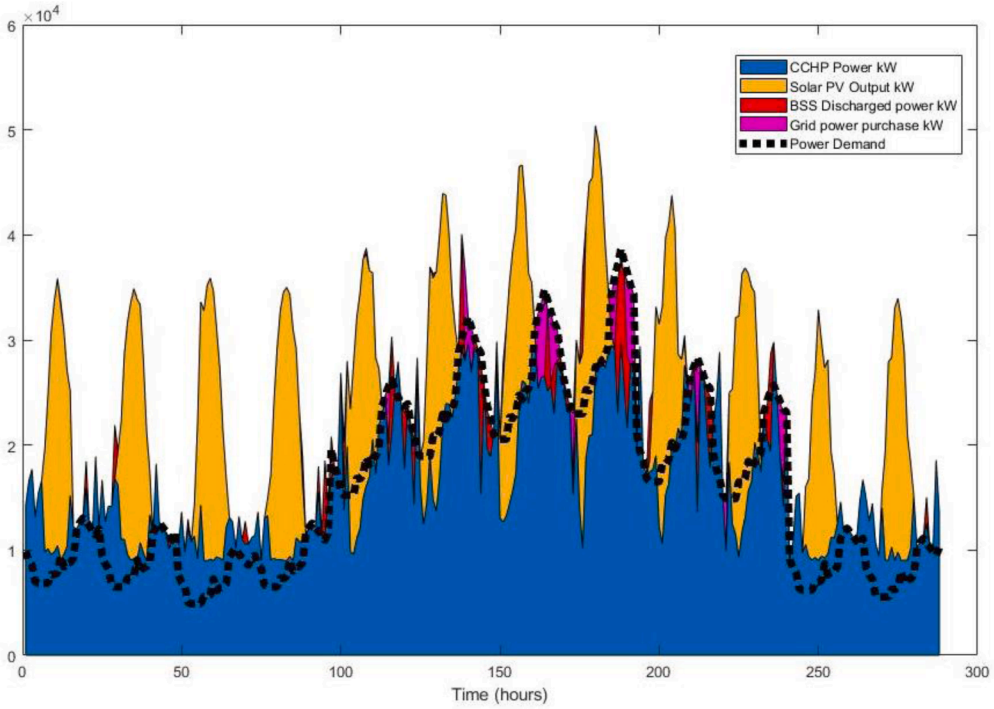

Fig. 15. Power balance-Scenario 2.

Fig. 10, the overall energy efficiency reduces as well as more useful heat is forced to be dumped.

Energy and exergy efficiency are inversely proportional in a nearly linear behavior while the dumped heat percentage from the total waste heat is following a non-linear increase as CCHP size increases. The program output reports the optimal value that gave highest profit then by increasing the capacity the results stabilized or diminishes, but due to randomness of the GA, many iterations have been made to observe the variation in results and the same is obtained.

This scenario yielded an optimal CCHP peak output power of 33 MW, 42.3 % and 66.4 % average exergy and energy efficiency, and 42.7% of the total waste heat is dumped and not utilized. Solar power contributed by 30% of the total generation, while 1.2% only is purchased from the Grid. The total cumulative profit for the 12 simulated days is 5.62 million EGP (0.36 million USD). As shown in Fig. 11, the CCHP is constantly operating most of the time but peaking in the summer (between time steps 100-200) to follow the thermal demand shown in Fig. 12.

5.1.2. Scenario 2: maximizing profit, Multiple CCHP sizes with AC Direct firing

In this scenario, the AC operates with high- and low-grade heat output from the CCHP with the ability to directly use natural gas to produce the required cooling output. The CCHP in this case is primarily driven by power demand, and it will dump the excess heat when it is forced to ramp up to minimize purchasing shortage in power from the

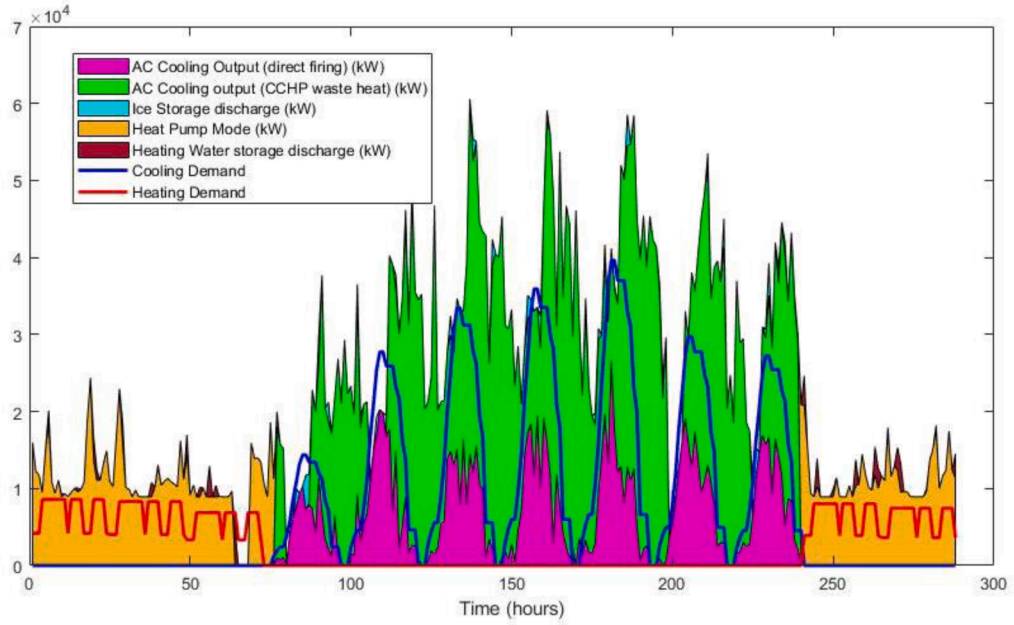

Fig. 16. Thermal balance-Scenario 2.

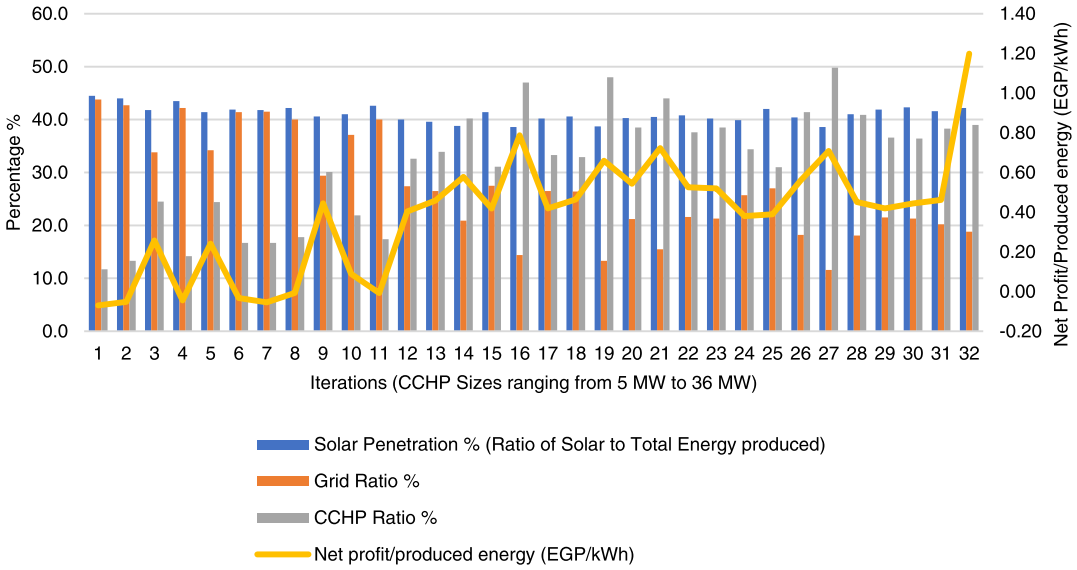

Fig. 17. Share of Power generation sources vs Profit Index-Scenario 3.

grid. It is found from the optimization results that 30 MW peak output of the CCHP gave the optimal profits, and yielded 39.3%, 68.41 % average exergy and energy efficiency respectively, and 41.2% average wasted heat. Solar power contributed by 32.3% of the total generation, and only 1.8% of the demand is purchased from the Grid.

As shown in Fig. 13, the profit follows a quadratic increase while CCHP capacities increase, almost like scenario 1 but in this scenario, the VPP achieved 5.39 million EGP (0.34 million USD), which is lower than scenario 1 due to the additional natural gas costs for firing the AC. Although 30 MW achieved the highest profit, it did not achieve the best economic index (shown in Fig. 14) due to higher purchase from the grid, thus, the lower total energy produced due to GA randomness. The power and thermal balance are illustrated in Fig. 15 and Fig. 16, respectively. In both scenarios 1 and 2, the contribution of TES tanks is minimal and surplus heat is being stored in Ice storage and heating storage tanks but without being discharged. Charing TES tanks involve additional costs; therefore, a scenario will be tested to evaluate the economic condition without including them. Exergy and energy efficiencies and dumped heat curves in this scenario are typically the same as Fig. 10 with slight variation in average values.

5.1.3. Scenario 3: Maximizing performance, Multiple CCHP sizes without AC Direct firing

In this scenario, the second multi-objective function is evaluated which drives the optimization to achieve optimal combined efficiency of energy and exergy efficiency. Since scenario 2 (without AC direct firing) achieved a 3% higher exergy efficiency than scenario 1, it is understood that the direct firing reduces the efficiencies, therefore this case is eliminated from the scenarios of maximization of performance. The optimization in this scenario selected 26 MW CCHP peak output. The calculated exergy and energy efficiencies are 38.5% and 63% respectively, and a significant low dumped heat of 10% is achieved. Although

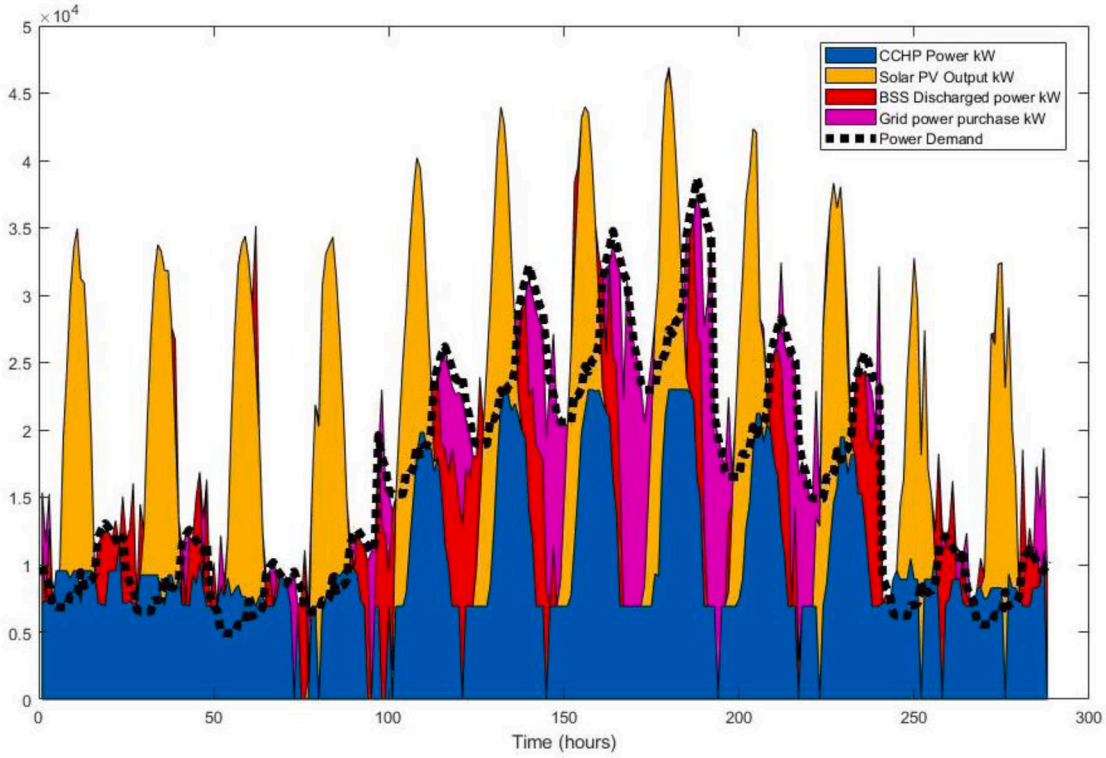

Fig. 18. Power balance-Scenario 3.

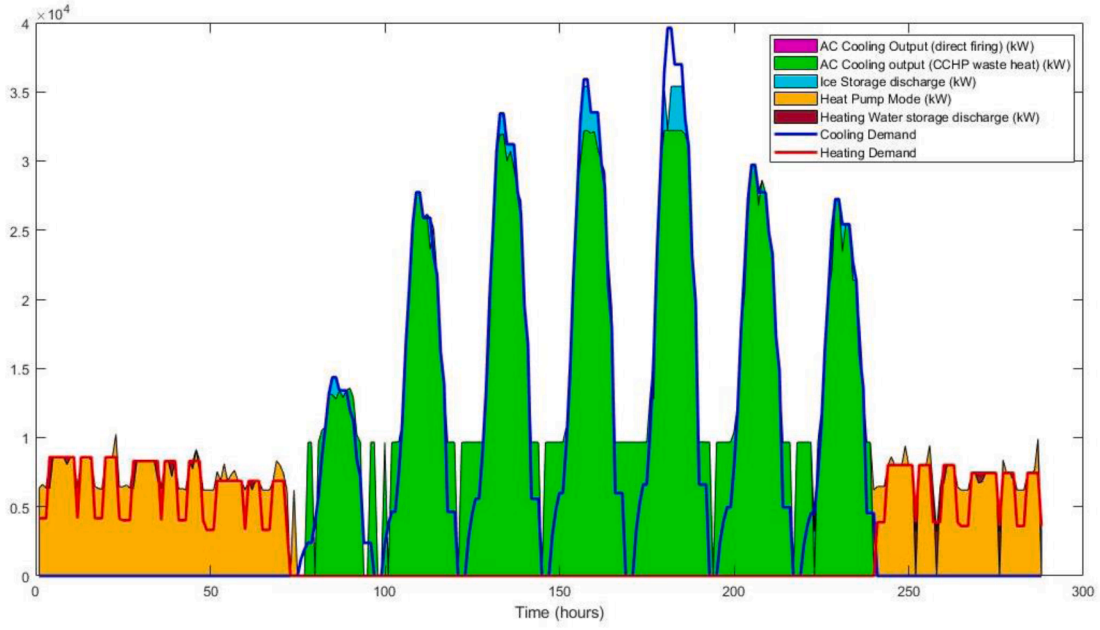

Fig. 19. Thermal balance-Scenario 3.

this performance is achieved, the profits are significantly lower than scenario 1 and 2 and estimated as 3.48 million EGP (0.22 million USD), with an economic index as 0.82 EGP/kWh which is comparable to scenario 1. From Fig. 17, it can be clear that this model increases the dependency on the grid, to reduce the power output from the CCHP and maximize the efficiencies, however, the first objective function (maximizing the profit) indirectly maintained a higher exergy and energy efficiencies although the dumped heat was higher.

Fig. 18 and Fig. 19 illustrates the power and thermal balance, from the figures it can be clear that the CCHP operation is interrupted at many time steps, once the AC is able to operate on its own fuel (e.g., time step: 70). Also, whenever solar power is dispatched, the CCHP shuts down. In this scenario, thermal balance constraint is converted to equality constraint instead of inequality as simulated in the previous scenarios, the operation is mainly following thermal demand as a priority of dispatch. With thermal balance equality constraint, the space cooling and heating demand are totally covered with minimal dumped heat. The average energy and exergy efficiencies achieved in this model are 38.5%

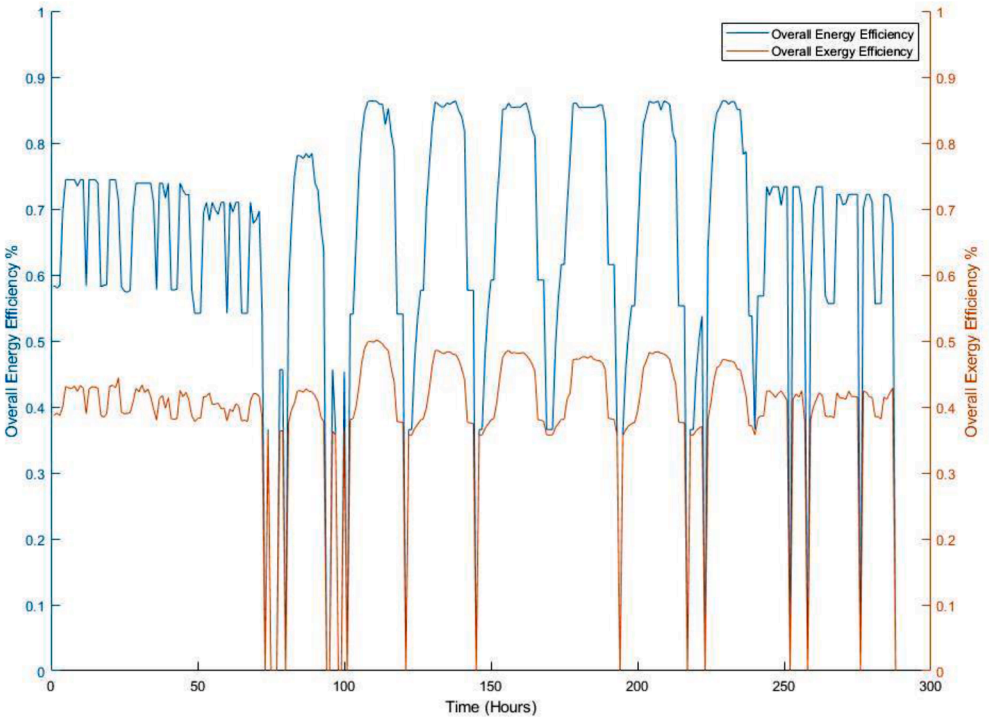

Fig. 20. Hourly energy and exergy efficiencies-Scenario 3.

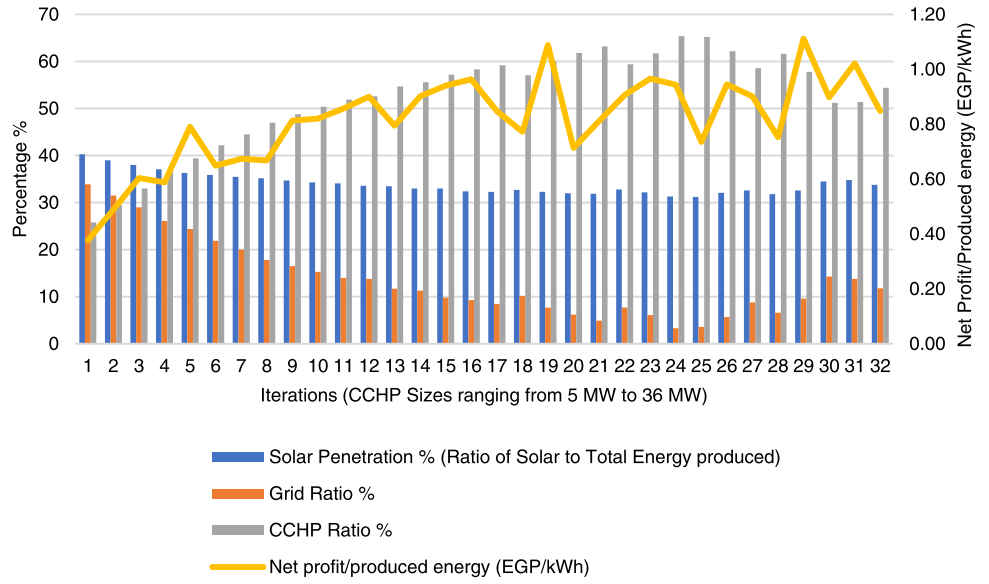

Fig. 21. Share of Power generation sources vs Profit Index-Scenario 4.

and 63% respectively, this average is lower than the first 2 scenarios, however, the lower values are due to multiple shutdowns of the plant, therefore, it is essential to assess the hourly efficiencies. As shown in Fig. 20, the energy and exergy efficiencies exceeded 42% and 80% respectively for around 55% of the time and exceeded 45% and 80% for around 20% of the time. These values signify that this model is highly efficient despite of the low achieved profit.

5.1.4. Scenario 4: Maximizing profit, Multiple CCHP sizes, without TES nor BSS, without AC Direct firing

Thermal storage tanks and BSS are excluded from this model, to evaluate their impact on the system profit and efficiency. This model achieved the optimal condition with 28 MW peak output power from the CCHP, 42.6% and 68.4 % exergy and energy efficiency, and 40% of total emitted heat is dumped to atmosphere. Solar power contributed by 31.3 % of the total generated power, while only 3.3 % is purchased from the grid. Emissions reduced by 47% compared to full dependency on the grid. Although these values could be comparable with Scenario 1, the capital costs and payback period are greatly reduced as will be explained in the summary part. Fig. 21 illustrates the share of power generation per technology, as shown, the grid dependency is at its minimum at 26–32 MW CCHP peak power, while solar power share reduction increases the profit index. Fig. 22 and Fig. 23 are illustrating the power and thermal balance. Unlike scenarios 1 and 2 where BSS contributed to coverage of the peak demand at time steps between 140-200, in this scenario, the peak demand is covered by the energy purchased from the

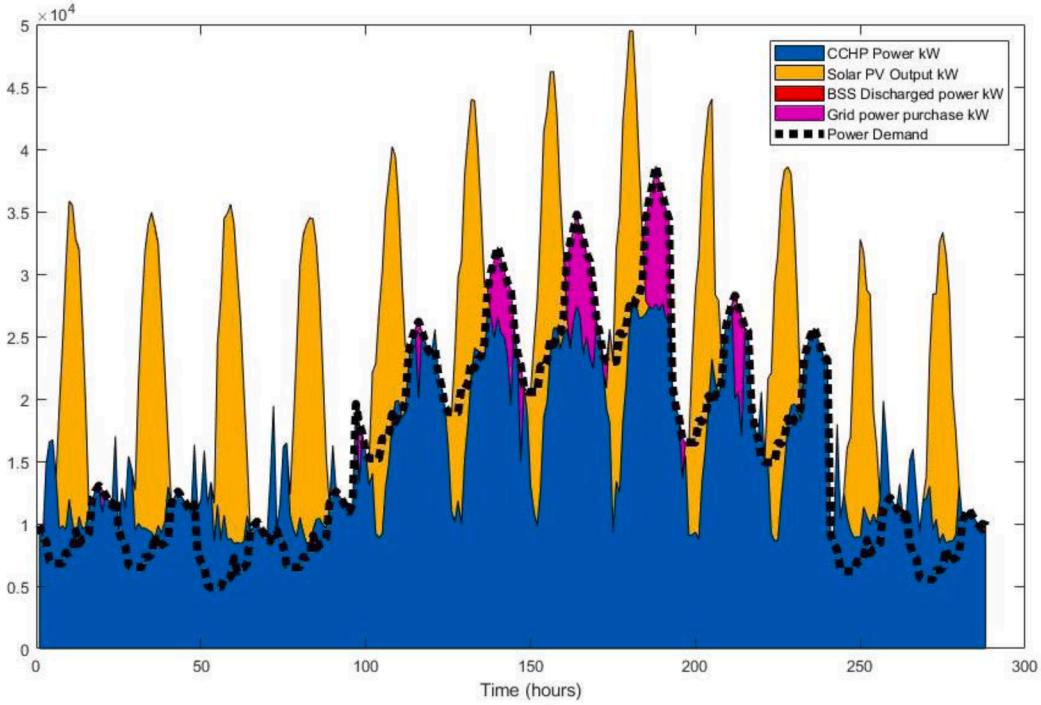

Fig. 22. Power balance-Scenario 4.

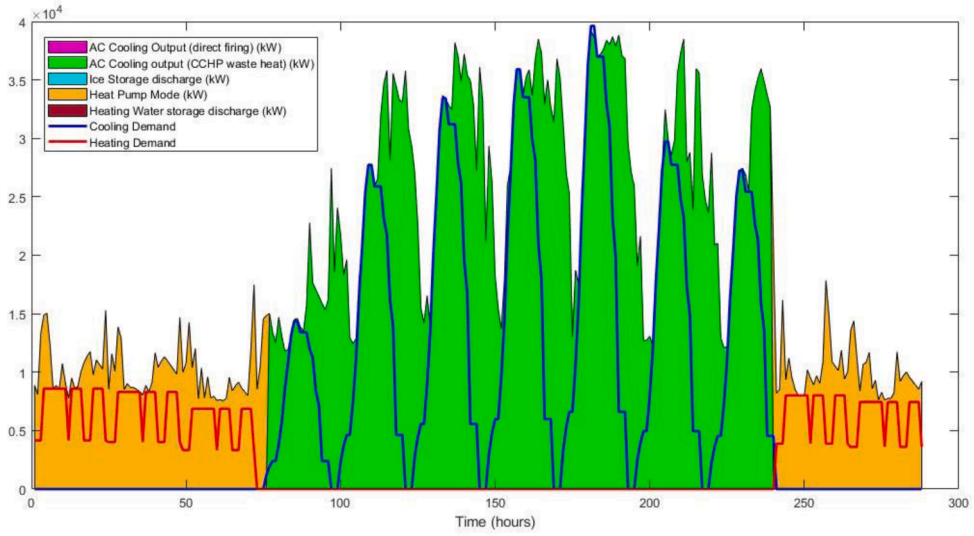

Fig. 23. Thermal balance-Scenario 4.

grid, which slightly reduced the overall profit.

5.1.5. Scenario 5: Maximize profit, Solar PV + BSS

In this scenario, the power demand is not excluding air conditioners load, it is assumed that solar PV and BSS will sell power to consumers at the public electricity tariff price and to the grid at the PPA price. It is found that the VPP in this case is achieving negative profit, which means that it purchases from the grid more than it sells to both consumers and to the grid. As shown in Fig. 24, it can be deducted that solar power was not enough in summer to be stored, and not enough to cover a full day in winter. This model would fit for consumer ownership of solar PVs to reduce his net electricity consumption and subsequently the energy bill, however, with the buildings' roof structure, it might be debatable whether all users (estimated as 144 appartements per building) could utilize the roof for this purpose, because from the power balance (Fig. 24) it is shown that in summer the solar PVs, although covering all roofs of the case study, partially cover the power demand and cannot respond to peaks even with BSS integration. This model should be studied separately with the announced Feed-in Tariff which is customized for energy consumers.

6. Results and discussion

For all VPP scenarios involving a CCHP plant that covers thermal demand, the consumer energy bill is 9% lower than the traditional case of being directly supplied with electricity from the grid. At the same time, the VPP models are achieving enough profit to break even with the power plants lifetime, Table 4 is illustrating the summary of the results

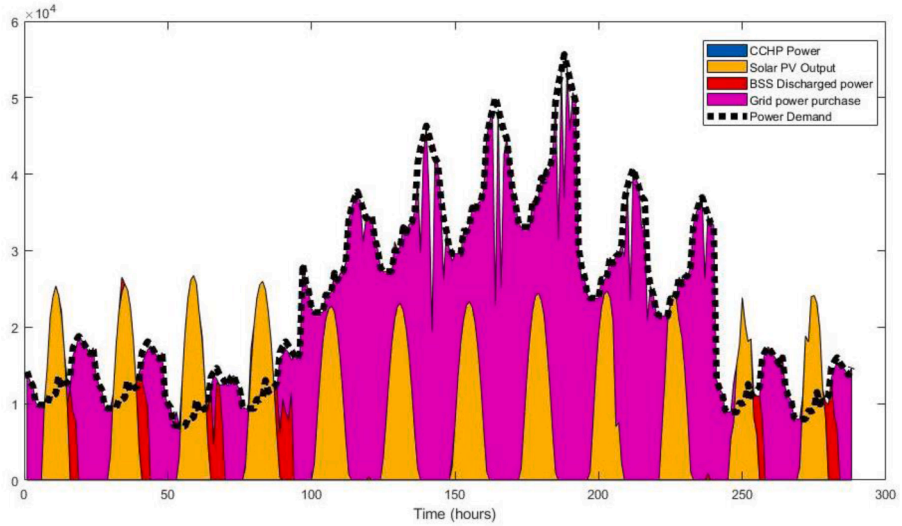

Fig. 24. Power balance-Scenario 5.

Table 4
Summary of results for 12 days.

Scenario	Revenues	Exergy Efficiency %	Energy Efficiency %	Dumped Heat %	Sold Energy to Grid (kWh)	Purchased Energy from Grid (kWh)	Solar Fraction %
0	-	-	-	-	-	5,280,363	
1	5,397,753	39.3	68.4	41.2	1,796,659	92,578	32.3
2	5,561,859	42.1	65.6	43.7	2,199,151	100,447	30.2
3	3,485,932	38.5	63	10	1,071,704	697,973	37
4	5,203,605	43	68	41	2,275,396	229,226	31.3
5	-4,086,229	-	-	-	207,177	4,463,086	32.5

Table 5
Capital costs.

System	Capital Cost	O&M Costs	Lifetime (years)	Reference
Gas Engine	1180 $/kW	0.02 $/kWh-year	25	(Zhang, et al., 2018)
Gas Fired Absorption Chiller	320 $/kW	0.01 $/kWh-year	25	(Zhang, et al., 2018)
Non-Fired Absorption Chiller	200 $/kW	0.01 $/kWh-year	25	(Zhang, et al., 2018)
Solar PV	190 $/kW	52.5 $/kW-year	25	(Jaganmohan, 2021) (Mundada, et al., 2016)
BSS	469 $/kWh	10 $/kW-year	15	(Mongird, et al., 2020) (Müller, et al., 2019)

for the 12 simulated days representing the full year in this study. The tradeoff between economic benefits and performance of the CCHP plant would be subjective to local environmental legislations. However, the economic benefits of the VPP would be more interesting for developers and the government itself which struggles to cover the increasing national electricity demand. The proposed VPP does not only provide economic benefits to itself and to the consumer, but it is also providing the national grid with 20-30% reserve from its total produced energy enough to cover the uncertainty and future increase of energy demand. In case the market undergoes another reform from regulated to liberated market, the VPPs will be able to trade in the ancillary services market and will relax the economic stress to build more conventional plants to follow the increase in future demand.

Economic assessment in terms of return on investment and payback period is analyzed, capital and O&M costs are illustrated in Table 5. A simple payback period is assessed to benchmark the economic feasibility of each VPP Model, as shown in Table 6, it is found that the model without storages and without AC direct firing option achieves a payback period of 18 years which is the lowest among the simulated models. This model also achieves the lowest dumped heat compared to other models following the maximum profit objective function.

While the other models following the multi-objective performance maximization objective function achieved a lower profit and a long payback period (39 years) which cannot break-even during the assumed project lifetime (25 years). Although achieved a long payback period, the optimal model achieved significant reduction in CO2 emissions, as shown in Table 6, compared to the reference case (scenario 0), which can be estimated as 47% annual savings.

To test the stability of the simulation of the most successful case (4) (having the lowest payback period), 30 runs of the same components sizes were performed and the worst, mediocre and best results were recorded. The judgement criteria is based on the achieved revenues as a priority, payback period and the newly introduced index (profit/produced energy) used to benchmark the models. Conceptually, this index (profit/produced energy) represents the value that the VPP should receive in average to break-even, which could be compared to the COE used in traditional approaches. Comparing the worse, mediocre and best results of case 4, the differences of revenues are fluctuating by +/- 2.5% which could prove the robustness of the model.

The results proved that the followed approach reduced the required cost of energy ($/kWh) by around 36% compared to the minimum achieved COE by literature. This improvement percentage could be furtherly improved by increasing thermal energy tariff and/or PPA

Table 6
Nominal sizes, payback period and CO2 emission values.

SCENARIOS	CCHP nominal size (MW)	Solar PV nominal Size (MW)	AC (MW)	BSS nominal size (MWh)	HW TES nominal (MWh)	CHW TES nominal (MWh)	Annual CCHP CO2 Emission (Tons)	Annual AC CO2 Emission (Tons)	Annual Grid CO2 Emission (Tons)	Total CO2 Emissions (Tons)	Revenues (EGP)	Profit/ produced energy (EGP/ kWh) (i.e., COE)	Payback Period (years)	
0. Reference Case: Total dependency on the Grid	-	-	-	-	-	-	-	-	146,213	146,213	-	-	-	
1. Max. Profit-With AC Firing-Dumped heat is allowed	69.7	233.5	28.5	160.5	50	35	71,008	1,164	2,563	74,737	5,397,753	0.8	26	
2. Max. Profit without AC Firing - Dumped heat is allowed	76.7	233.5	28.5	160.5	77	21	77,852	0.0	2,781	80,633	5,561,859	1.1	23	
3. Max. Performance without Ac Firing Dumped heat is minimized	46.5	233.5	28.5	160.5	156	116	49,574	0.0	19,327	68,901	3,485,932	0.8	39	
4. Max. Profit without AC Firing without Storages – Dumped heat is allowed	65	233.5	28.5	-	-	-	72,622	0.0	6,649	79,272	5,173,228	1.04	19.1	Worst
	65	233.5	28.5	-	-	-	74,132	0.0	5,488	79,621	5,307,151	1.05	18.9	Medicore
	65	233.5	28.5	-	-	-	71,803	0.0	5,852	77,655	5,440,993	1.09	18.2	Best
5. Max Profit-only Solar PV	-	233.5	-	61.8	-	-	-	-	123,583	123,583	-4,086,229	-1.90	-	

Table 7
COE found in literature and equivalent systems description.

Reference	COE ($/kWh)
(Abo-Elyousr & Elnozahy, 2018)	0.538
(Diab, et al., 2019)	0.218
(Diab, et al., 2016)	0.19
(Elkadeem, et al., 2020)	0.15
(Dawoud, et al., 2015)	0.139
(El-Sattar, et al., 2021)	0.339
(El-Sattar, et al., 2021)	0.11

selling price to grid. In comparison with relevant literature, the optimal configuration achieved an economic index (i.e., COE) of 1.09 EGP/kWh (0.07 $/kWh) (using a currency rate of 1 USD = 15.7 EGP) is lower than the COE values found in relevant papers as shown in Table 7. The adopted approach in this study proved to provide more realistic results and more controllable in term of operation management and energy efficiency estimation. Although tariff structure could vary from country to country, but the same approach could be applicable in other countries. As a generalization concept for the ratio of capacities needed to satisfy the load, a normalization for the required energy production capacities satisfying a unit of energy demand is performed. Based on the results, 1 kWh electricity demand is covered by energy to be produced from:

31% solar power + 65% CCHP + 4% Grid

The estimated system sizes signifies that to achieve optimal profit, efficiency and reduce grid dependency, the percentage of CCHP size to Solar PVs nominal capacities are found as 22:78, and that the CCHP should not be sized based on peak load, instead, the peak load should be covered by the grid power. This capacity percentage will be useful as an index for future studies attempting to improve the payback period.

This study have the following limitations that would require further work:

- The grid interaction is based on “pay as generated” concept of PPA, other PPA structures could change the results
- Future energy demand increase is not addressed in this study, it is questionable whether expansion of the proposed model is needed or would it be able to ramp-up to cover the demand.
- The solar PVs are modelled on the concept of maximizing all available roof-spaces attempting to maximize the deployment of solar power. It is questionable whether partial utilization of rooftop spaces for solar PVs deployment (by means of reducing capital cost) would yield profitable results or reduce the payback period. Nevertheless, Using the same maximization concept (utilizing the roofs) would be able to respond to future expansion of the residential blocks. In case more blocks are built, more rooftop areas would be available for expanding solar PVs areas, but higher capacity of CCHP will be required.
- Non-linearity of part-load efficiency of CCHP consideration in such an aggregated operation of power plants is a matter of question. This consideration pushes for the need of GA or similar stochastic solvers, however, using alternative approach of converting the non-linearity with piecewise linearization would enable the usage of Mixed Integer Linear Programming which is more stable. Such a comparison will be needed to prove the usefulness of non-linearity consideration within a combined group of operating power plants.
- Future devaluation of the local currency which will affect the predefined-electricity tariff needs to be furtherly considered.

7. Conclusion

This paper investigated a new modeling approach of VPPs’ design and operation in regulated markets considering selling power and

thermal energy to consumers and surplus to electricity grids through PPA. The modeling approach consisted of tailoring a profit maximization objective function complying with the PPA rules and existing electricity tariff structure. The solution yields the optimal configuration of the VPP that achieve minimum payback period. The main findings could be summarized as follows:

- The adopted approach reduced the cost of energy needed for the VPP to break-even by 36% compared to the minimum COE achieved by literature.
- The integration of BSS with the current capital costs is not economically beneficial as it increases the payback period by 4-5 years. The simulation proved to be better to directly consume or export the generated power to the grid.
- The proposed method showed that solar power contributed by around 31% of the total generated power. Grid dependency consisted of approximately 4%. CO2 emissions reduced by 47% compared to full dependency on the grid.
- The results showed that energy and exergy efficiencies are not directly proportional to profit achievement. In terms of performance, it is shown that allowing heat to be dumped, although it wastes useful heat resource to the atmosphere is more economically viable for the hybrid system and it contributed to the reduction of TES Sizes as also found in other studies (Mongibello, et al., 2015). Aggregating more residential clusters having their own VPPs, may utilize this dumped heat and improve the system performance.

Further work is necessary to create a comprehensive understanding of the energy pricing in Egypt and demand modeling and its impact on VPPs, this shall include the following:

- Energy demand accurate modeling in term of profiles, consumption values and uncertainty of future demand
- Comparing the solutions achieved with GA against other algorithms to verify its stability.
- District energy pricing based on time-of-use rather than fixed tariff.
- Alternative electricity tariff synthesizing based on time-of-use.
- Integration of consumer as a contributor to VPP components (e.g., as owners of solar PVs) and studying profit sharing scheme and how this idea would impact the profitability, payback period and energy bill.
- Simulation of multiple residential clusters contributing to energy trading as multiple VPPs.
- Running more cases on consecutive days in winter or summer for analyzing the variation of SOC level and inter-seasonal modeling of the storage systems based on a full year hourly demand.

Declaration of Competing Interest

The authors declare that they have no known competing financial interests or personal relationships that could have appeared to influence the work reported in this paper.

References

Abo-Elyousr, F. K., & Elnozahy, A. (2018). Bi-objective economic feasibility of hybrid micro-grid systems with multiple fuel options for islanded areas in Egypt. *Renewable Energy, 128*(1), 37–56.

Aldali, K. M., & Moustafa, W. S. (2016). An attempt to achieve efficient energy design for High-Income Houses in Egypt: Case Study: Madenaty City. *International Journal of Sustainable Built Environment, 5*(2), 334–344.

Alipour, M., Zare, K., & Mohammadi-Ivatloo, B. (2014). Short-term scheduling of combined heat and power generation units in the presence of demand response programs. *Energy, 71*(1), 289–301.

Arsalis, A. (2012). *Integration of a heat pump subsystem to a residential high temperature PEMFC micro-CHP System.* Perugia, Italy: ECOS.

Attia, S., Evrard, A., & Gratia, E. (2012). Development of benchmark models for the Egyptian residential buildings sector. *Applied Energy, 94*(1), 270–284.

Barakat, S., Samy, M., Eteiba, M. B., & Wahba, W. I. (2016). *Viability study of grid connected PV-Wind-Biomass hybrid energy system for a small village in Egypt.* Cairo. In *2016 Eighteenth International Middle East Power Systems Conference (MEPCON)*.

Bellini, E., 2019. *First private PPA for utility-scale solar in Egypt is signed.*[Online] Available at: https://www.pv-magazine.com/2019/01/21/first-private-ppa-for-utility-scale-solar-in-egypt-is-signed [Accessed 02 May 2021].

Calvillo, C. F., Sánchez-Miralles, A., Villar, J., & Martín, F. (2016). Optimal planning and operation of aggregated distributed energy resources with market participation. *Applied Energy, 182*(1), 340–357.

Cano, A., Arévalo, P., & Jurado, F. (2020). Energy analysis and techno-economic assessment of a hybrid PV/HKT/BAT system using biomass gasifier: cuenca-Ecuador case study. *Energy, 202*(1), 1–16.

Darrow, K., Tidball, R., Wang, J., & Hampson, A. (2017). *Catalog of CHP technologies.* Washington: U.S. Environmental Protection Agency Combined Heat and Power Partnership.

Dawoud, S. M., et al. (2015). Feasibility Study of Isolated PV-Wind Hybrid System in Egypt. *Advanced Materials Research, 1092*(1), 145–151.

Deb, K. (2001). *Multi-objective optimization using evolutionary algorithms* (1 ed.). New York: John Wiley & Sons, Inc.

Deng, J., Wang, R., & Han, G. (2011). A review of thermally activated cooling technologies for combined cooling, heating and power systems. *Progress in Energy and Combustion Science, 37*(2), 172–203.

Diab, A. A. Z., Sultan, H. M., & Kuznetsov, O. N. (2019). Optimal sizing of hybrid solar/wind/hydroelectric pumped storage energy system in Egypt based on different meta-heuristic techniques. *Renewable Energy And Water Sustainability*, 1–23.

Diab, F., Lan, H., Zhang, L., & Ali, S. (2016). An environmentally friendly factory in Egypt based on hybrid photovoltaic/wind/diesel/battery system. *Journal of Cleaner Production, 112*(1), 3884–3894.

Dio, V. D., et al. (2015). Critical assessment of support for the evolution of photovoltaics and feed-in tariff(s) in Italy. *Sustainable Energy Technologies and Assessments, 9*(1), 95–104.

Egypt Independent, 2021. *Egypt's Electricity Ministry institutes new pricing structure.* [Online] Available at: https://egyptindependent.com/egypts-electricity-ministry-institutes-new-pricing-structure/ [Accessed 02 May 2021].

Elkadeem, M., et al. (2020). A systematic decision-making approach for planning and assessment of hybrid renewable energy-based microgrid with techno-economic optimization: A case study on an urban community in Egypt. *Sustainable Cities and Society, 54*(1), 1–26.

El-Sattar, H. A., et al. (2021). Optimal design of stand-alone hybrid PV/wind/biomass/battery energy storage system in Abu-Monqar, Egypt. *Journal of Energy Storage, 44*(A), 1–20.

EU Science Hub, 2019. *Photovoltaic Geographical Information System.*[Online] Available at: https://re.jrc.ec.europa.eu/pvg_tools/en/#MR [Accessed 19 April 2021].

Foroughi, M., Pasban, A., Moeini-Aghtaie, M., & Fayaz-Heidari, A. (2021). A bi-level model for optimal bidding of a multi-carrier technical virtual power plant in energy markets. *Electrical Power and Energy Systems, 125*(1), 1–12.

Google Earth. (2020). *Google Earth.* Google. s.l.

Green, C., & Garimella, S. (2021). Residential microgrid optimization using grey-box and black-box modeling methods. *Energy and Buildings, 235*(1), 1–14.

Hadayeghparast, S., Farsangi, A. S., & Shayanfar, H. (2019). Day-ahead stochastic multi-objective economic-emission operational scheduling of a large scale virtual power plant. *Energy, 172*(1), 630–646.

Hasan, M. I., & Jabbar, E. K. (2021). Fabricating and testing of the ground coupled air conditioner for residential applications in Iraqi weather. *Energy, 216*(1), 1–10.

Hermans, M., & Delarue, E. (2016). *Impact of start-up mode on flexible power plant operation and system cost.* Porto, Portugal. In *2016 13th International Conference on the European Energy Market (EEM)*.

Herrera, F., & Magdalena, L. (1997). Genetic fuzzy systems: A tutorial. *Tatra Mt. Math. Publ.(Slovakia), 13*, 93–121.

Jaganmohan, M., 2021. *Quarterly prices of solar photovoltaic multi modules in the United States from 1st quarter 2016 to 3rd quarter 2020.*[Online] Available at: https://www.statista.com/statistics/216791/price-for-photovoltaic-cells-and-modules/ [Accessed 26 April 2021].

Kamel, M. A., Elbanhawy, A. Y., & El-Nasr, M. (2019). A novel methodology to compare between side-by-side photovoltaics and thermal collectors against hybrid photovoltaic thermal collectors. *Energy Conversion and Management, 202*(1), 1–20.

Kamel, M. A., Elbanhawy, A. Y., & El-Nasr, M. A. (2021). Quantification of deviations between grey-box and constant efficiency modeling and optimization of trigeneration systems using a data-driven RMSD indicator. *Sustainable Energy Technologies and Assessments, 45*(1), 1–16.

Kasaei, M. J., Gandomkar, M., & Nikoukar, J. (2017). Optimal management of renewable energy sources by virtual power plant. *Renewable Energy, 114*(1), 1180–1188.

Kolhe, M., Agbossou, K., Hamelin, J., & Bose, T. (2003). Analytical model for predicting the performance of photovoltaic array coupled with a wind turbine in a stand-alone renewable energy system based on hydrogen. *Renewable Energy, 28*(5), 727–742.

Koutroulis, E., Kolokotsa, D., Potirakis, A., & Kalaitzakis, K. (2006). Methodology for optimal sizing of stand-alone photovoltaic/wind-generator systems using genetic algorithms. *Solar Energy, 80*(1), 1072–1088.

Ko, W., & Kim, J. (2019). Generation expansion planning model for integrated energy system considering feasible operation region and generation efficiency of combined heat. *energies, 12*(226), 1–20.

Kumara, K. P., Saravanana, B. & Swarupb, K., 2015. *A Two Stage Increase-Decrease Algorithm To Optimize Distributed Generation In a Virtual Power Plant.* Mumbai, s.n.

Liu, M., Shi, Y., & Fang, F. (2013). Optimal power flow and PGU capacity of CCHP systems using a matrix modeling approach. *Applied Energy, 102*(1), 794–802.

Alhamid, M. I., et al. (2020). Operation strategy of a solar-gas fired single/double effect absorption chiller for space cooling in Indonesia. *Applied Thermal Engineering, 178*(1), 1–14.
Maleki, A., Hafeznia, H., Rosen, M. A., & Pourfayaz, F. (2017). Optimization of a grid-connected hybrid solar-wind-hydrogen CHP system for residential applications by efficient metaheuristic approaches. *Applied Thermal Engineering, 123*(1), 1263–1277.
Mandal, S., Das, B. K., & Hoque, N. (2018). Optimum sizing of a stand-alone hybrid energy system for rural electrification in Bangladesh. *Journal of Cleaner Production, 200*(1), 12–27.
Martinopoulos, G., & Bassiliades, N. (2019). Electricity markets with increasing levels of renewable generation: structure, operation, agent-based simulation, and emerging designs. Fernando Lopes, Helder Coelho (Eds.), Springer, Cham (2018), ISBN: 978-3-319-74261-8 *Energy, 186*(1), 1–2.
McGreevy, D. M., et al. (2021). Expediting a renewable energy transition in a privatised market via public policy: The case of south Australia 2004-18. *Energy Policy, 148*(A), 1–14.
Mohammadi, M., Musa, S. N., & Bahreininejad, A. (2014). Optimization of mixed integer nonlinear economic lot scheduling problem with multiple setups and shelf life using metaheuristic algorithms. *Advances in Engineering Software, 78*(1), 41–51.
Mondal, D., Chakrabarti, A., & Sengupta, A. (2020). *Power system small signal stability analysis and control* (Second ed.). Cambridge, Massachusetts: Academic Press Inc.
Mongibello, L., N, B., Caliano, M., & Graditi, G. (2015). Influence of heat dumping on the operation of residential micro-CHP. *Applied Energy, 160*(1), 206–220.
Mongird, K., et al. (2020). An evaluation of energy storage cost and performance characteristics. *Energies, 13*(1), 1–51.
Moussawi, H. A., Fardoun, F., & Louahlia, H. (2017). Selection based on differences between cogeneration and trigeneration in various prime mover technologies. *Renewable and Sustainable Energy Reviews, 74*(1), 491–511.
Müller, N., et al. (2019). Energy storage sizing strategy for grid-tied PV plants under power clipping limitations. *energies, 12*(1), 1–17.
Mundada, A., Shah, K., & Pearce, J. (2016). Levelized cost of electricity for solar photovoltaic,battery and cogen hybrid systems. *Renewable and Sustainable Energy Reviews, 57*(1), 692–703.
Next Kraftwerke, 2021. *What is a virtual power plant?*.[Online] Available at: https://www.next-kraftwerke.com/knowledge/what-is-a-virtual-power-plant [Accessed 04 May 2021].
Nezamabadi, H., & Nazar, M. S. (2015). Arbitrage strategy of virtual power plants in energy, spinning reserve and reactive power markets. *IET Generation, Transmission & Distribution, 10*(3), 750–763.
Nosratabadi, S. M., Hooshmand, R.-A., & Gholipour, E. (2017). A comprehensive review on microgrid and virtual power plant concepts employed for distributed energy resources scheduling in power systems. *Renewable and Sustainable Energy Reviews, 67*(1), 341–363.
NREL, 2021. *Solar Levelized Cost of Energy Analysis*.[Online] Available at: https://www.nrel.gov/solar/solar-levelized-cost.html [Accessed 02 May 2021].
Paidipati, J., Frantzis, L., Sawyer, H., & Kurrasch, A. (2008). *Rooftop Photovoltaics Market Penetration Scenarios*. Massachusetts: National Renewable Energy Laboratory.
Pandžić, H., Morales, J. M., Conejo, A. J., & Kuzle, I. (2013). Offering model for a virtual power plant based on stochastic programming. *Applied Energy, 105*(1), 282–292.
Ramli, M. A., Bouchekara, H., & Alghamdi, A. S. (2018). Optimal sizing of PV/wind/diesel hybrid microgrid system using multi-objective self-adaptive differential evolution algorithm. *Renewable Energy, 121*(1), 400–411.
Ren, H., Gao, W., & Ruan, Y. (2008). Optimal sizing for residential CHP system. *Applied Thermal Engineering, 28*(1), 514–523.
RE-Source, 2020. *Risk mitigation for corporate renewable PPAs*.[Online] Available at: https://windeurope.org/intelligence-platform/product/risk-mitigation-for-corporate-renewable-ppas/ [Accessed 17 April 2022].
Tabassum, M., & Mathew, K. (2014). A Genetic Algorithm Analysis towards Optimization solutions. *International Journal of Digital Information and Wireless Communications, 4*(1), 124–142.
UKCOP26, 2021. *COP26 GOALS*.[Online] Available at: https://ukcop26.org/cop26-goals/ [Accessed 19 December 2021].
Wang, J.-J., Jing, Y.-Y., Zhang, C.-F., & Zhai, Z. (2011). Performance comparison of combined cooling heating and power system Performance comparison of combined cooling heating and power system. *Applied Energy, 88*(1), 4621–4631.
Wang, J., Lu, Y., Yang, Y., & Mao, T. (2016). Thermodynamic performance analysis and optimization of a solar-assisted combined cooling, heating and power system. *Energy, 115*(1), 49–59.
Wang, J., & Wu, J. (2015). Investigation of a mixed effect absorption chiller powered by jacket water and exhaust gas waste heat of internal combustion engine. *International Journal of Refrigeration, 50*(1), 193–206.
Wang, J.-J., Yang, K., Xu, Z.-L., & Fu, C. (2015). Energy and exergy analyses of an integrated CCHP system with biomass air gasification. *Applied Energy, 142*(1), 317–327.
Xu, Y., Liu, Z., Wen, F., & Palu, I. (2021). Receding-horizon based optimal dispatch of virtual power plant considering stochastic dynamic of photovoltaic generation. *Energy Conversion and Economics, 2*(1), 45–53.
Zamani, A. G., Zakariazadeh, A., & Jadid, S. (2016). Day-ahead resource scheduling of a renewable energy based virtual power plant. *Applied Energy, 169*(1), 324–340.
Zeng, A., et al. (2020). Research on real-time optimized operation and dispatching strategy for integrated energy system based on error correction. *energies, 13*(2908), 1–21.
Zeng, R., et al. (2016). A novel multi-objective optimization method for CCHP–GSHP coupling systems. *Energy and Buildings, 112*(1), 149–158.
Zhang, H., Xie, Z., Lin, H.-C., & Li, S. (2020). Power capacity optimization in a photovoltaics-based microgrid using the improved artificial bee colony. *Applied sciences, 10*(9), 1–21.
Zhang, J., Cao, S., Yu, L., & Zhou, Y. (2018). Comparison of combined cooling, heating and power (CCHP) systems with different cooling modes based on energetic, environmental and economic criteria. *Energy Conversion and Management, 160*(1), 60–73.
Zheng, C. Y., Wu, J. Y., & Zhai, X. Q. (2014). A novel operation strategy for CCHP systems based on minimum distance. *Applied Energy, 128*(1), 325–335.
Zhoua, Z., et al. (2013). Impacts of equipment off-design characteristics on the optimal design and operation of combined cooling, heating and power systems. *Computers and Chemical Engineering, 48*(1), 40–47.